Complete solutions to the problem of quantisation errors arising from digital measurements of a repeated square wave signal

Andrea Capotorti
Department of Mathematics and Statistics
University of Bologna, Bologna, Italy
and
Frank Lad
Department of Mathematics and Statistics
University of Canterbury[1], *Christchurch, New Zealand*

No. 150 December, 1996

Abstract – This report documents the complete solutions to the problem of representing the posterior distribution for the pulse width modulation of a repeated square wave signal based on digital measurements of the duration of the on and the off components of the waves.

[1] Thanks to a University of Canterbury research grant for computational support.

Introduction

The information content of an on-off electrical pulse is encoded in the pulse width modulation of the squarewave signal, defined as the ratio τ/T of the "on" time component of the square wave, τ, relative to the full period (on plus off time) of the pulse, T. The reports of Lad and Dunlop (1996a, 1996b) have described the problem of making inferences about the pulse width modulation of a squarewave signal when the durations of its on and off components are measured by discrete beat counts of a vibrating crystal. The present report relies on these two for describing the physical setup that generates the observations and for describing the logic of deriving the posterior distributions for τ/T given digital counts of on and off durations of single signal wave and of a repeated wave. We shall refer to these reports as Report 1 and Report 2 when needed to identify specific information required to read the present report.

Report 2 has identified the limited array of observation sequences denoted by $\{M_1, N_1, M_2, N_2\}$ that can possibly be observed when a second signalling wave is an exact replica of the first. An explicit derivation of the posterior distribution for τ/T is presented for the case when the conditioning values of $M_1 < M_2$ and $N_1 < N_2$, specifically for the Region of the unit-cube we have labelled 2C1. It is only promised that a complete presentation of the results of similar analyses for the remaining cases will appear in a technical monograph. The present report contains these promised results.

While specific details of the analysis are different within each Region of the unit-cube, the groundwork for deriving each part of the solution is similar in structure. We have capitalised on this by writing main sections of the programs using variable names x, y, z,and Q, and replacing these with specifics appropriate to each particular Region being studied. In this way, the format of our analysis resembles that followed in Report 1 which solved the single wave signal problem in generic terms, rather than Report 2 which solved the repeated signal problem in terms quite specific to Regions 1C1 and 2C1 of the unit-cube.

Figure 0.1 will make this idea precise, straight away. Each Region of the unit-cube defined in Table 1 of Report 2, is characterised firstly by an ordering of the values of $\epsilon_0, \epsilon_\tau$, and ϵ_T. Then the Region is made more precise by locating the position of ϵ_1, which is defined in terms of ϵ_0 and ϵ_T, within this ordering. In this way, the structure of all Region definitions is similar, even though the details of the orderings are quite different in their implications for the solution. Figure 1 shows the unit-cube in dimensions labelled (x, y, z). To ease visualization we shall always be concerned with the sixth-section for which $x < y < z$. For any particular region we would be studying, the three epsilons change places in being represented by x, y, and z. You will remember from Report 2 that the propagation equation for ϵ_1 in the second wave represents this by $\epsilon_1 = \epsilon_0 - \epsilon_T + (\epsilon_0 < \epsilon_T)$. The various subregions are then determined by moving the position of ϵ_1 through the various possible orderings within this order of (x, y, z). The variable Q will be used to represent the quotient τ/T, which is always

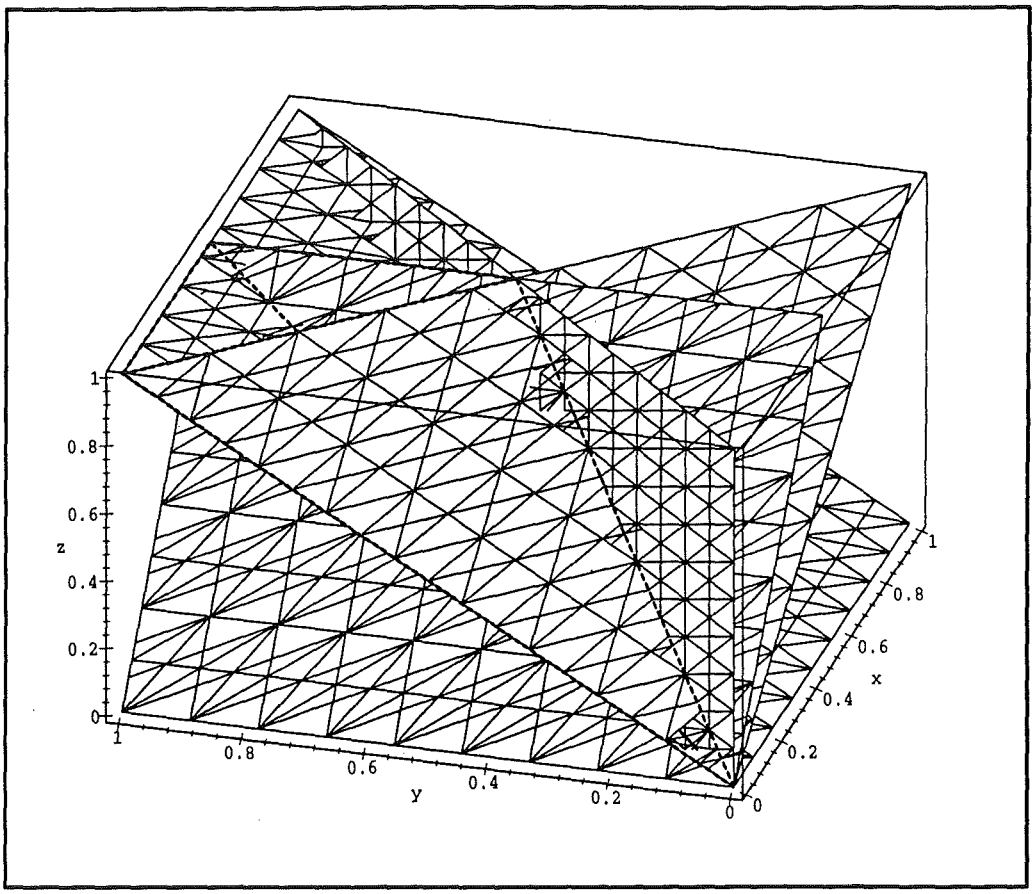

Figure 0.1: The unit-cube representing possible values of $\epsilon_T < \epsilon_\tau < \epsilon_0$ via $x < y < z$, for the subregion we designate by 2C2. The planes defined by $z = 2x$ and $z = x + y$ determine the bounding Region, by the ordering of $\epsilon_1 = z - x$ between x and y. Edges of Region 2C2 are identified by dark dashed lines.

defined as some rational function of ϵ_τ, and ϵ_T. Thus, in the developments of the present paper, the equations will always involve Q as a function of two components of the triple (x, y, z).

The Region considered in Figure 1 is 2C, in which $\epsilon_T < \epsilon_\tau < \epsilon_0$, these three playing the roles of x, y, and z, respectively. So the propagation equation reduces to $\epsilon_1 = z - x$. Now in Region $2C2$, for example, ϵ_1 is restricted to lie between x and y, yielding the linear inequalities $z > 2x$, and $z < x + y$. These planes appear in Figure 1, so this region 2C2 can be viewed accordingly. Once the joint density of the epsilons has been integrated over values of z, that is ϵ_0, this region is projected down into the space of (x, y) for further analysis which will be detailed in Section 2 of this Report. Figures of subdivisions of the unit-cube relevant to the other Regions of the cube appear in Appendix A.

For organisational purposes, we divide the various conditioning structures for the data sequence $\{M_1, N_1, M_2, N_2\}$ into three Categories. Category I solutions pertain to data conditions that are met only within a single Region of the unit-cube. From Table 2 of Report 2, this will be recognised as the condition of $M_1 < M_2$ and $N_1 = N_2$, which is satisfied only within Region 2C2, and the condition $M_1 > M_2$ and $N_1 = N_2$, satisfied only in Region 1A2. For shorthand terminology we think of these observation

conditions as "UPEQ" and "DNEQ" respectively, for hopefully obvious reasons. This naming convention will be followed throughout this report when it is convenient. As can be recognised again in Table 2 of Report 2, Category II solutions are those which are each satisfied by conditions pertaining in two Regions: UPUP in 1C1 and 2C1; EQUP in 1C2 and 2B1; EQDN in 1B2 and 2A2; and DNDN in 2A3 and 1A3. Finally, a Category III solution is merited only in the observation condition of EQEQ, but it occurs within 6 Regions: 1A1, 1B1, 1C3, 2A1, 2B2, and 2C3.

Each Category of the solution has its own unique form of complexity. It turns out that when conditions are such to make some feature of a solution simple within one category of conditioning data, other features of the solution for that case become more complex. This will be observed as we go.

Category I solutions

Each of the cases 2C2 where $M1 < M2$ and $N1 = N2$ and 1A2 where $M1 > M2$ and $N1 = N2$ occur within only one region of the unit cube. Thus, to determine the expression of the density $f(Q|M1, M2, N1, N2)$, for this Category of solution there is no need to derive a weighted mixture density over different regions.

The analysis of these two cases is quite similar. For this reason we shall discuss their common aspects in general terms, and for the particular computations and plots we shall refer only to Region 2C2 where $M1 < M2$ and $N1 = N2$. The prior probability of each Region is $1/24$, derived by integrating the uniform density over the appropriate section of the unit-cube.

The simplicity of these cases with respect to the other two Categories of solution is only apparent. In fact, in each of these two single regions, the boundary planes for ϵ_0, that is z, (defined in terms of x and y) change four times, as can be see in the plots in Figure 0.1 and in Figure A.1 of Appendix A. For this reason, the boundary specifications for the integral with respect to ϵ_0 of $f(\epsilon_0, \epsilon_\tau, \epsilon_T|M1, M2, N1, N2, Region)$ differ, and this leads to four different algebraic expressions for the joint density of ϵ_τ and ϵ_T.

Figure 0.2 then displays the projection of region 2C2, through the z dimension, that is the ϵ_0 dimension, into the space of (x, y), divided into four parts: part a corresponds to the boundaries x, $2x$ and $1 - x$; part b corresponds to the boundaries $2x$ and $1 - x$; part c corresponds to the boundaries $1 - x$, $2x$ and 1; and part d corresponds to the boundaries $1 - x$, $2x$ and 1. Subdividing the Region into four parts is necessary to perform the margining integration to derive the conditional density $f(Q|M1, M2, N1, N2, Region)$, since in each part the joint density $f(\epsilon_\tau, \epsilon_T|M1, M2, N1, N2, Region)$ has a different algebraic expression.

These four parts of the projection of 2C2 are transformed into the domain $T(2C2)$ (in Figure 0.3) according to the equation $Q = (a-1+2x)/(b+2y)$. (We regularly use the simplified notation prescribing $a = M_1+M_2$, and $b = N_1+N_2$. The boundary lines in T(2C2) are determined by the transformations of the five lines $l1, l2, l3, l4, l5$ and by the line $y = 1$ which bound the Region 2C2 shown in Figure 0.2. The transformed Region appears in Figure 0.3. Despite the fact that these transformations are rational functions, the transformed lines appear to be straight in the Figure only because the relevant domain of Q is so tiny.

The computation of the margining integration follows exactly the same steps done for the region 2C1 in Report 2 Section 4.2: the joint density of Q and y is generated by applying the variable transformation

$$(x, y) \longrightarrow (Q, y) : Q = (a - 1 + 2x)/(b + 2y) \tag{0.1}$$

to the joint of x and y (ϵ_T and ϵ_τ) and multiplying it by the Jacobian of the inverse transformation; the marginal density for Q is derived by integrating this joint with respect to y. Boundary limits on the integration (varying among $l1\prime$, $l2\prime$, $l3\prime$, $l4\prime$, $l5\prime$ and 1 (see Figure 0.3)) must be specified distinctly over four intervals of the domain of Q, each interval identified by two nodal points.

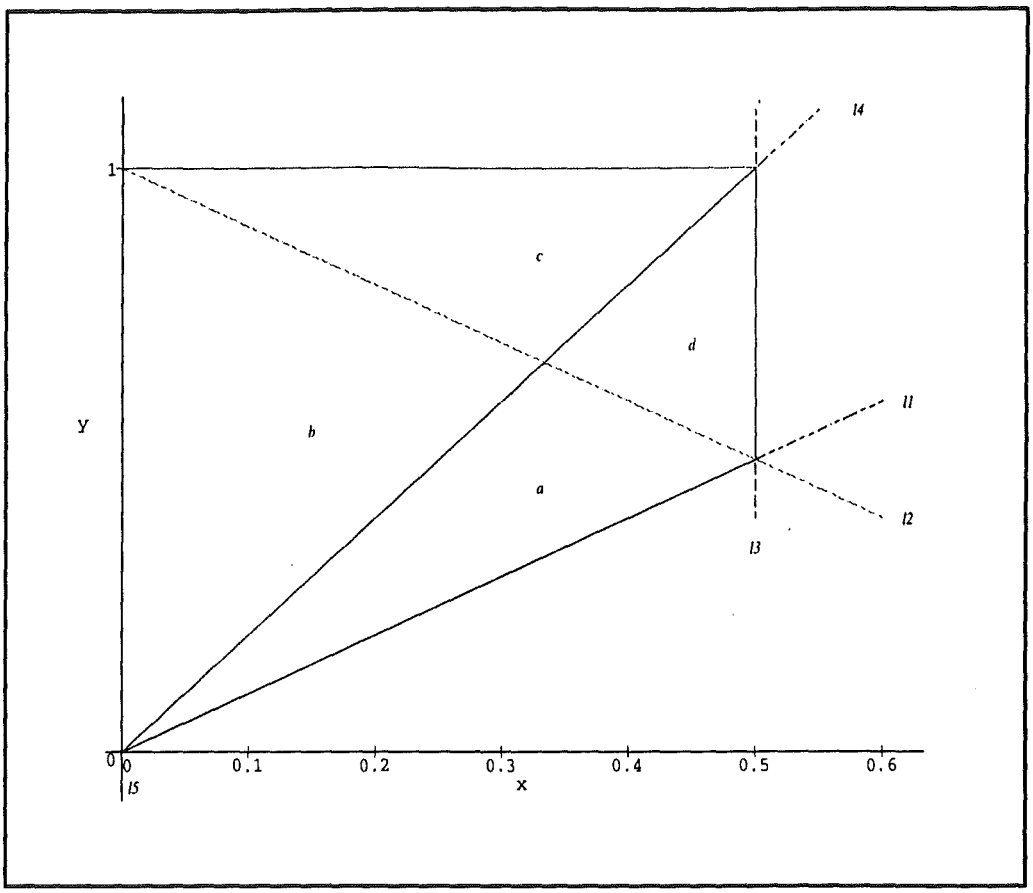

Figure 0.2: Projection of Region 2C2 in the space (x, y).

In the MAPLE programs the explicit expressions of the boundaries of the integration and of the nodal points are never explicitly seen, because it is possible to use the implicit form of the transformation of the lines in the (x, y) plane by means of equation 0.1.

For $T(2C2)$ the nodal points are

$$(a-1)/b < a/(b+1) < a/b < (a+1)/(b+1) < (a+1)/b \tag{0.2}$$

where, remember, $a = M1 + M2$ and $b = N1 + N2$.

In each interval, different parts of $T(2C2)$ are involved with their different expression of the joint density. Ultimately, in each interval the density is a rational function of Q and, considering the entire domain of Q, it is continuous, but with a discontinuous second derivative.

For two pulses derived from a measurement at 0 C degrees (icepoint), the mean, the variance and the standard deviation have the following values:

$$\begin{aligned} E(Q|M1 = 233, M2 = 234, N1 = N2 = 725) &= 0.3221302957 \\ \text{although } \frac{M1+M2}{N1+N2} &= 0.3220689655 \\ V(Q|M1 = 233, M2 = 234, N1 = N2 = 725) &= 0.602 \cdot 10^{-7} \\ SD(Q|M1 = 233, M2 = 234, N1 = N2 = 725) &= 0.2453 \cdot 10^{-3} \end{aligned}$$

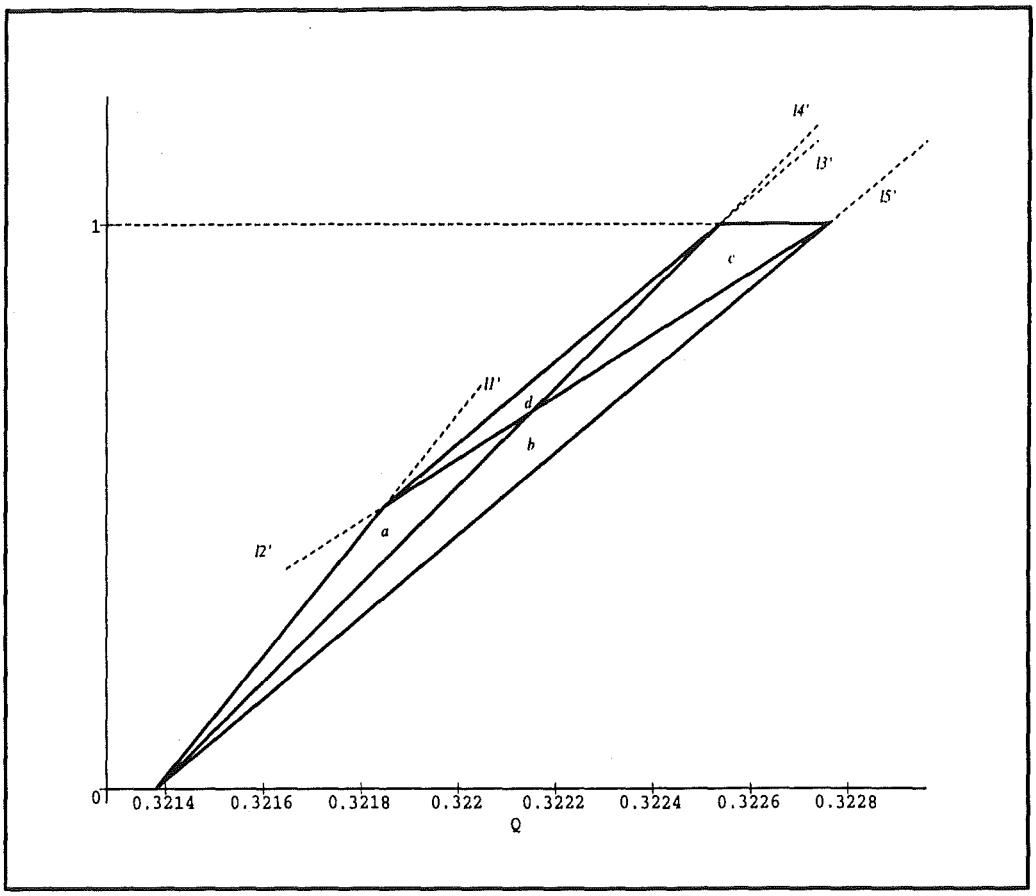

Figure 0.3: $T(2C2)$ is a transformation of the domain 2C2 by $(x, y) \longrightarrow (Q, y)$, specified in equation 0.1.

The dark curve in Figure 0.4 displays the density function under the condition of observing $M1 = 233$, $M2 = 234$, $N1 = N2 = 725$. For comparative purposes the dashed line plots a normal density with the same mean and variance.

Figure 0.5 displays the density function again as a dark curve, and shows separately the four functions deriving from integration over the parts of $T(2C2)$ whose sum yields this desired density.

The shape of the density depends on the value of the ratio $(M1+M2)/(N1+N2)$. In fact, the relative distances among the nodal points displayed in equation 0.2 change as the numerical value of a changes. In Figure 0.6 three "extreme" densities are displayed corresponding to the values of the ratio a/b equal to .95, .50, and .05, translated to the same location so the extent of their differences in skewness can be observed. Differences in the skewness exhibited by each are due to the different relative positions of the nodal points and the consequent "shifting" of the functions resulting from integrating the four parts of $T(2C2)$. Note that when $a = b/2$ the density is perfectly symmetric. The Figures displayed in Appendix B show corresponding graphs relevant to the other category I solution found in Region 1A2.

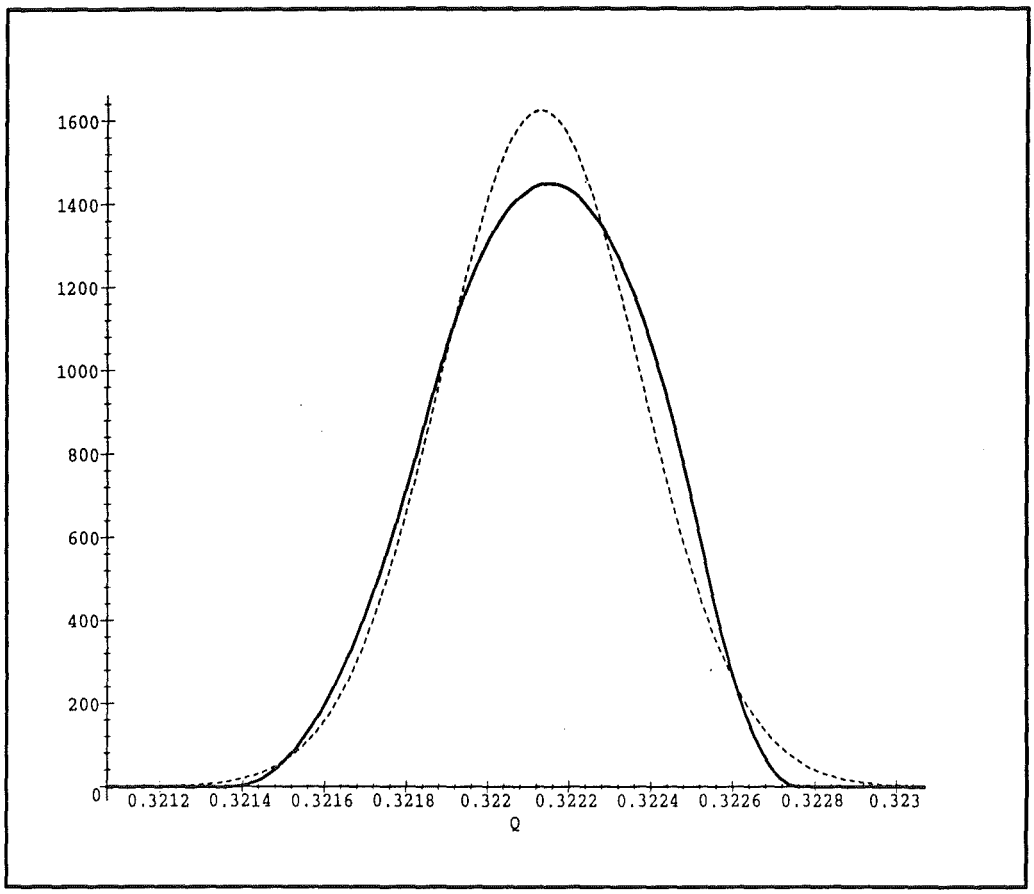

Figure 0.4: The density function $f(Q|M1 = 233, M2 = 234 N1 = N2 = 725)$ appears as the solid black curve. For comparative purposes, the dashed curve plots a normal density with the same mean and variance: $N(0.3221302957, 0.602 \cdot 10^{-7})$.

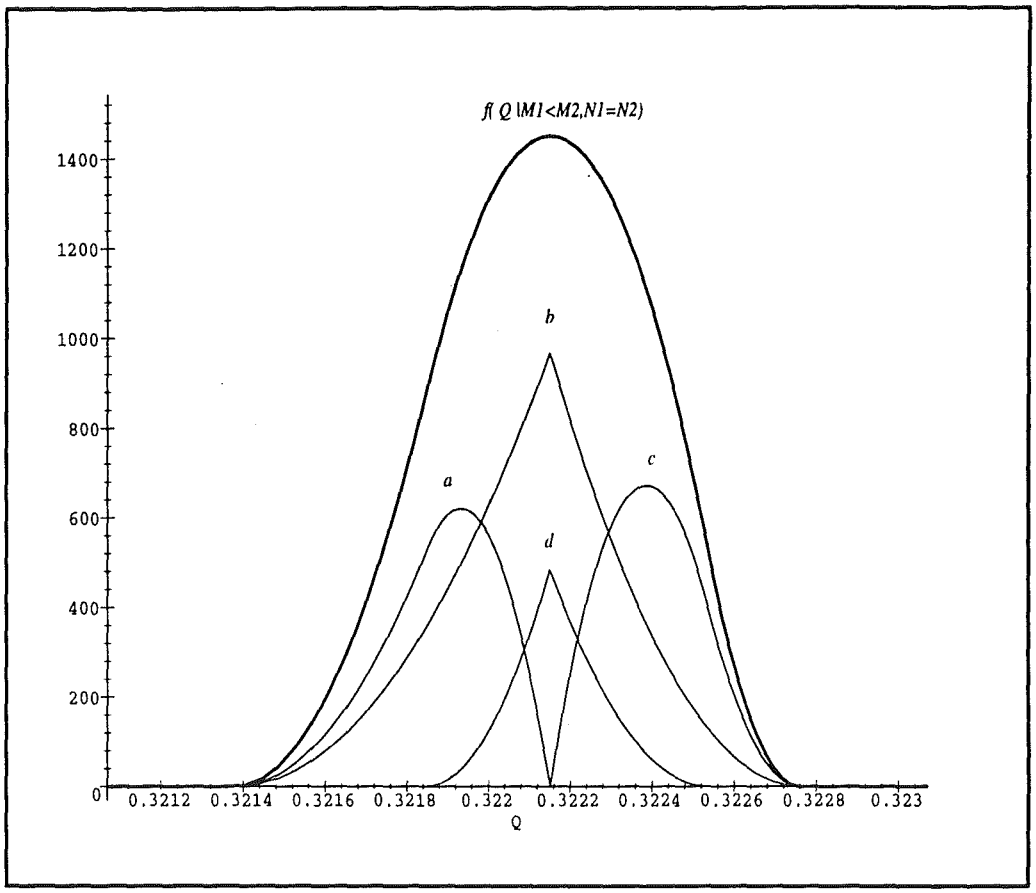

Figure 0.5: The density function $f(Q|M1 = 233, M2 = 234, N1 = N2 = 725)$ and the four contributing component functions derived by integrating the joint density over the parts a, b, c, and d of Figure 0.3.

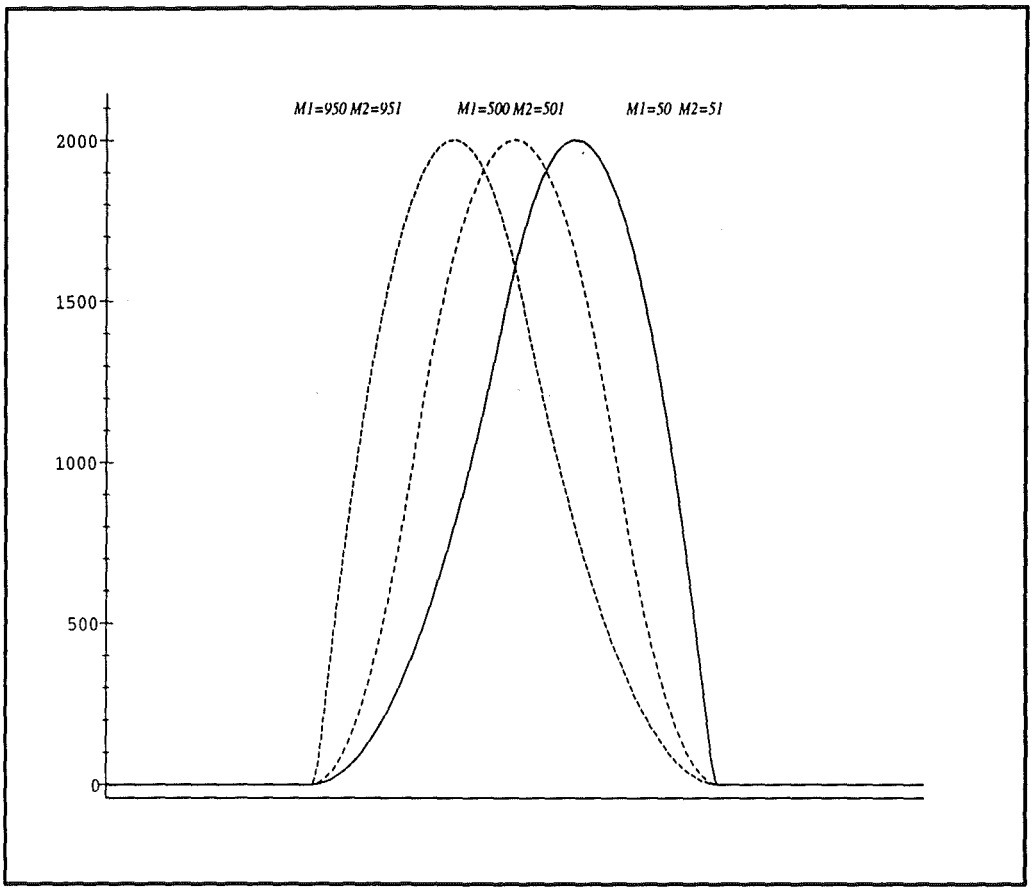

Figure 0.6: Three different shapes for $f(Q|M1 < M2, N1 = N2)$ with $N1 = N2 = 1000$.

Category II solutions

The second Category of solutions pertains to those cases whose conditioning data can occur when the epsilon vector lies within two different regions of the unit-cube.

In Table 0.1 the four cases of data structure corresponding to this Category, along with their defining regions are shown. The first case ($M1 < M2$ and $N1 < N2$) is

	Cases	Regions
UPUP	$M1 < M2$ and $N1 < N2$	1C1 and 2C1
EQUP	$M1 = M2$ and $N1 < N2$	1C2 and 2B1
EQDN	$M1 = M2$ and $N1 > N2$	1B2 and 2A2
DNDN	$M1 > M2$ and $N1 > N2$	1A3 and 2A3

Table 0.1: Cases with two regions.

that one fully described in Report 2.

The analyses of all these cases have strong analogies both in the characters of the regions (the boundaries for ϵ_0 change twice) and in the characters of the final distributions. The cases UPUP and DNDN yield densities with similar shapes but with opposite skewness; the same holds for cases EQUP and EQDN. Moreover, the cases of UPUP and EQUP yield similar densities to those displayed in Figure 0.7 which displays three density shapes for EQUP, but the shapes corresponding to the ratios of $(M_1 + M_2)/(N_1 + N_2)$ change places at the low and high end of the spectrum. For these reasons, for numerical and graphical examples we shall display in this Section the densities corresponding to the case EQUP.

As mentioned before, for each region involved in these cases, the boundaries for ϵ_0 change twice (see the relevant Figures for these sections of the unit-cube in Appendix A). The procedure to determine $f(Q|M1, M2, N1, N2, Region)$ is exactly the same as for Categor I cases (with the obvious difference that now the number of parts of each subregion with distinct algebraic forms of density are two and not four) and it is fully described in Report 2, Table 2.

Once $f(Q|M1, M2, N1, N2, Region)$ is obtained for both the regions of each case, a weighted sum is necessary to determine the density function $f(Q|M1, M2, N1, N2)$. The weights used in summing the two pieces are the prior probabilities of each region as they are listed in Report 2.

Figure 0.7 displays the density for the Case EQUP obtained with two pulses observed at 0 C degree (icepoint). The thin lines represent the densities in regions 1C2 and 2B1; the fat line is the mixture of the two and hence it displays the density appropriate to the entire case. For comparison, the dashed line represent a normal

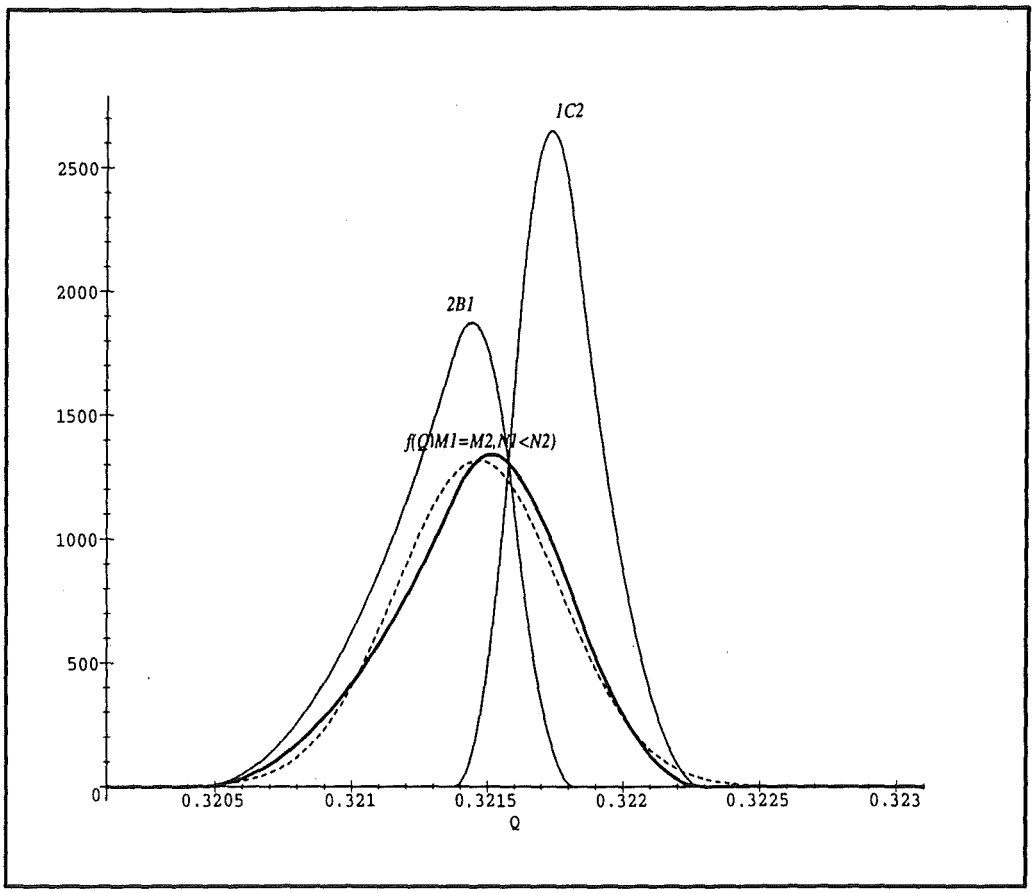

Figure 0.7: The density function $f(Q|M1 = M2 = 233, N1 = 724, N2 = 725)$ appears as the fat solid line. The densities conditional within regions 1C2 and 2B1 appear as the thin solid lines, and for comparative purposes, the dashed line plots a normal density $N(0.3214655246, 0.919 \cdot 10^{-7})$.

density with same mean and variance as $f(Q|M1 = 233, M2 = 233, N1 = 724, N2 = 725)$.

For two pulses derived from a measurement at 0 C degree (icepoint), the mean, the variance and the standard deviation have the following values:

$$\begin{aligned} E(Q|M1 = M2 = 233, N1 = 724, N2 = 725) &= 0.3214655246 \\ \text{although } \frac{M1 + M2}{N1 + N2} &= 0.3216011042 \\ V(Q|M1 = M2 = 233, N1 = 724, N2 = 725) &= 0.919 \cdot 10^{-7} \\ SD(Q|M1 = M2 = 233, N1 = 724, N2 = 725) &= 0.3031 \cdot 10^{-3} \end{aligned}$$

For these cases too, the shape of the density depends on the numerical value of the ratio $\frac{M1 + M2}{N1 + N2}$ which causes different relative distances among the nodal points and the consequent modification of the mixture. For each region there are four nodal

points, but three of them are shared in common between the two regions involved in each case. Thus, as shown in equation 0.3 for case EQUP, there are five nodal points in total.

$$\left.\begin{array}{lccccc} 1C2nodes & & \frac{a}{b+1} & \frac{a}{b} & \frac{a}{b-1} & \frac{a+1}{b} \\ 2B1nodes & \frac{a-2}{b-1} & \frac{a}{b+1} & \frac{a}{b} & \frac{a}{b-1} & \end{array}\right\} \Rightarrow \frac{a-2}{b-1} < \frac{a}{b+1} < \frac{a}{b} < \frac{a}{b-1} < \frac{a+1}{b} \tag{0.3}$$

In Figure 0.8 three "extreme" densities are displayed, corresponding at the values

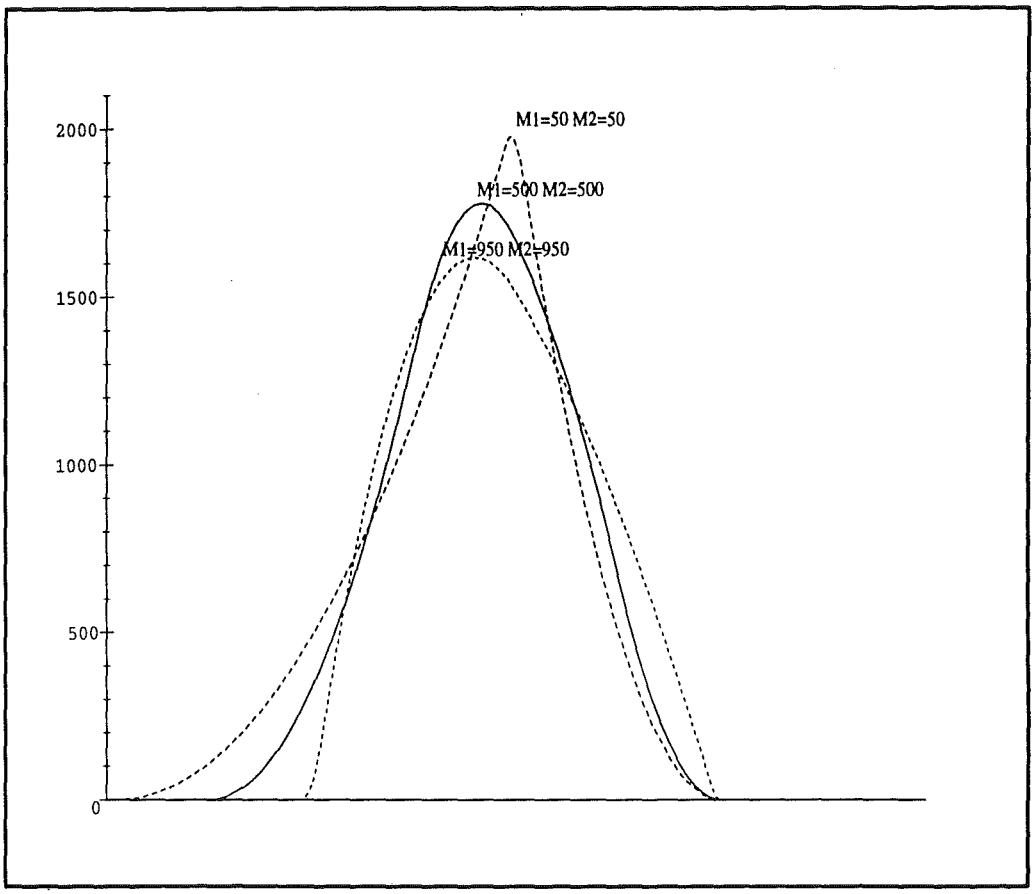

Figure 0.8: Three different shapes for $f(Q|M1 = M2, N1 < N2)$ with $N1 = 1000$ and $N2 = 1001$

$a = 100$, $a = 1000$ and $a = 1900$ with a fixed value $b = 2001$. Note that contrary to Category I displayed in Figure /refequptwo, for this Category the shape of the density and the domain of Q change a lot over this range. Moreover, a configuration of exact symmetry is never reached since the constraint $a < b$ does not allow a symmetric position for the nodal points.

Category III solutions

The last Category for the possible observation structures occurs only for the case of $M1 = M2$ and $N1 = N2$ (EQEQ). This case involves six different regions of the unite cube (1A1, 1B1, 1C3, 2A1, 2B2 and 2C3) but in each region the boundaries for ϵ_0 remain fixed. So the bigger complexity for the number of regions is, in such a way, "counterpoised" by an easier analysis required in each region.

The procedure to obtain $f(Q|M1 = M2, N1 = N2)$ follows exactly the same steps reported in Report 1 for $f(Q|M1, N1)$. For this reason we will not show the details here.

In each region the joint distribution $f(\epsilon_\tau, \epsilon_T|M1 = M2, N1 = N2, Region)$ is obtained integrating the uniform density respect to ϵ_0 with bondary determined by the planes that identify the region. Later the transformation

$$Q = \frac{a - 2 + (\epsilon_0 \geq \epsilon_\tau) + (\epsilon_1 \geq \epsilon_\tau) + 2\epsilon_\tau}{b - 2 + (\epsilon_0 \geq \epsilon_T) + (\epsilon_1 \geq \epsilon_T) + 2\epsilon_T} \tag{0.4}$$

is applied to obtain the joint density of Q with ϵ_T or with ϵ_τ and, at the end, it is marginalized.

The final density is obtained as a weighted mixture of the six densities arising within the regions. Again, the weights of the mixture are the prior probabilities shown Table 2 in of Report 2. Figure 0.9 shows these six densities and the mixture of them (dark curve) for an observation of $M1 = M2 = 233$ and $N1 = N2 = 725$.

The set of the nodal points for the final density is the union of the nodal points for the several regions. All these points are listed in Table 0.2.

Regions	Nodal points		
1A1	$\frac{a-2}{b}$	$\frac{a-1}{b-1}$	$\frac{a}{b}$
1B1	$\frac{a}{b}$	$\frac{a}{b-1}$	$\frac{a+2}{b}$
1C3	$\frac{a}{b+1}$	$\frac{a}{b}$	$\frac{a+1}{b+1}$
2A1	$\frac{a-1}{b-1}$	$\frac{a}{b}$	$\frac{a}{b-1}$
2B2	$\frac{a-2}{b}$	$\frac{a}{b+1}$	$\frac{a}{b}$
2C3	$\frac{a}{b}$	$\frac{a+1}{b+1}$	$\frac{a+2}{b}$

Table 0.2: Nodal points for the case $M1 = M2$ and $N1 = N2$.

The union of all these points has cardinality seven and the order depends of the

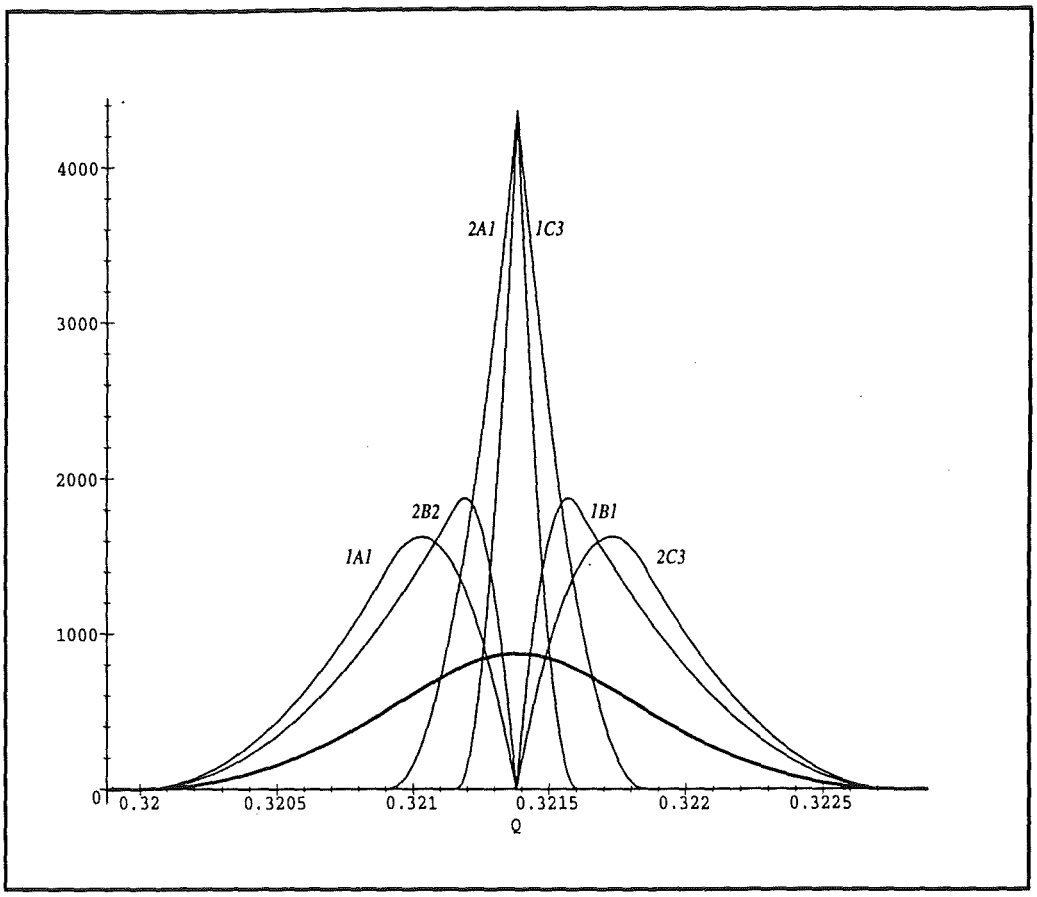

Figure 0.9: $f(Q|M1 = M2 = 233, N1 = N2 = 725)$ appears as the fat solid line, the densities on regions 1A1, 1B1, 1C3, 2A1, 2B2 and 2C3 appear as the thin solid lines.

relative magnitude of the quantity a respect to b. In fact we have:

$$\begin{cases} \frac{a-2}{b} < \frac{a-1}{b-1} < \frac{a}{b+1} < \frac{a}{b} < \frac{a}{b-1} < \frac{a+1}{b+1} < \frac{a+2}{b} & \text{if} \quad a \leq \frac{b-1}{2} \\ \frac{a-2}{b} < \frac{a-1}{b-1} < \frac{a}{b+1} < \frac{a}{b} < \frac{a+1}{b+1} < \frac{a}{b-1} < \frac{a+2}{b} & \text{if} \quad \frac{b-1}{2} \leq a \leq \frac{b+1}{2} \\ \frac{a-2}{b} < \frac{a}{b+1} < \frac{a-1}{b-1} < \frac{a}{b} < \frac{a+1}{b+1} < \frac{a}{b-1} < \frac{a+2}{b} & \text{if} \quad \frac{b+1}{2} \leq a \end{cases} \tag{0.5}$$

For two signal observed at 0 C degree (icepoint) with $M1 = M2 = 233$ and $N1 = N2 = 725$ the mean, the variance and the standard deviation have the following values:

$$\begin{aligned} E(Q|M1 = M2 = 233, N1 = N2 = 725) &= 0.3213792985 \\ \text{although } \frac{M1+M2}{N1+N2} &= 0.3213793103 \\ V(Q|M1 = M2 = 233, N1 = N2 = 725) &= 0.2042 \cdot 10^{-6} \\ SD(Q|M1 = M2 = 233, N1 = N2 = 725) &= 0.4519 \cdot 10^{-3} \end{aligned}$$

Figure 0.10 displays the density conditional on these observations along with a normal density with the same mean and variance (dashed line). Note that in this case

$f(Q|M1, M2, N1, N2)$ is very close to a normal density, almost indistinguishable, but there are two main differences: $f(Q|M1 = M2, N1 = N2)$ is perfectly symmetric only when $\frac{b-1}{2} \leq a \leq \frac{b+1}{2}$; otherwise there is a little skewness since the nodal points do not have a symmetric distribution with respect the central point $\frac{a}{b}$. (This can be deduced from equation 0.5.) From a theoretical point of view, the normal distribution allows Q to have values on all the real line (also outside the interval $[0, 1]$!). On the contrary the domain of $f(Q|M1 = M2, N1 = N2)$ is $\left[\frac{a-2}{b}, \frac{a+2}{b}\right]$. Nonetheless, the normal distribution puts virtually 0 probability outside this same interval.

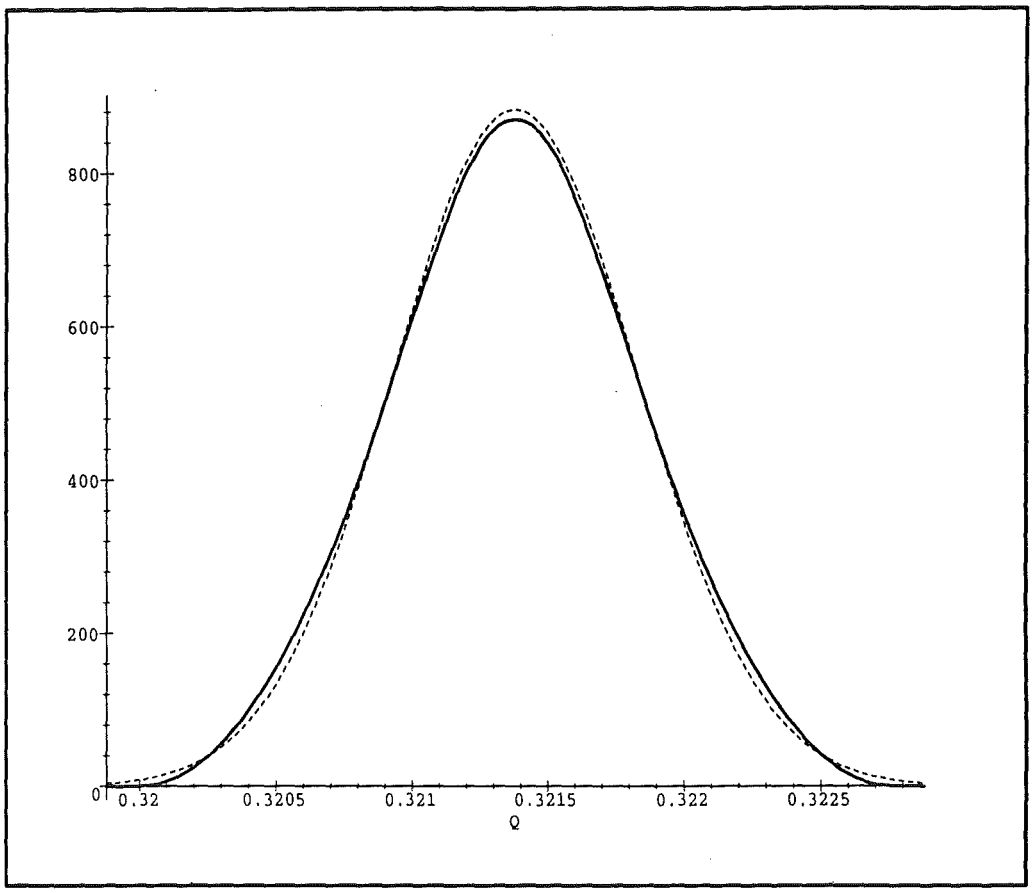

Figure 0.10: $f(Q|M1 = M2 = 233, N1 = N2 = 725)$ appears as the solid line and, for comparative purposes, the dashed line plots a normal density $N(0.3213792985, 0.2042 \cdot 10^{-6})$.

In this case the density has the same symmetry property found in Report 1 for a single measured pulse, i.e.

$$f(Q|M1 = M2 = m, N1 = N2 = n) = f(1 - Q|M1 = M2 = n - m, N1 = N2 = n) \tag{0.6}$$

For this reason in Figure 0.11, where three different shapes are shown for $N1 = N2 = 1000$, the maximum used value is $a = \frac{b}{2}$, for bigger values of a the shapes repeat themselves according to equation0.6.

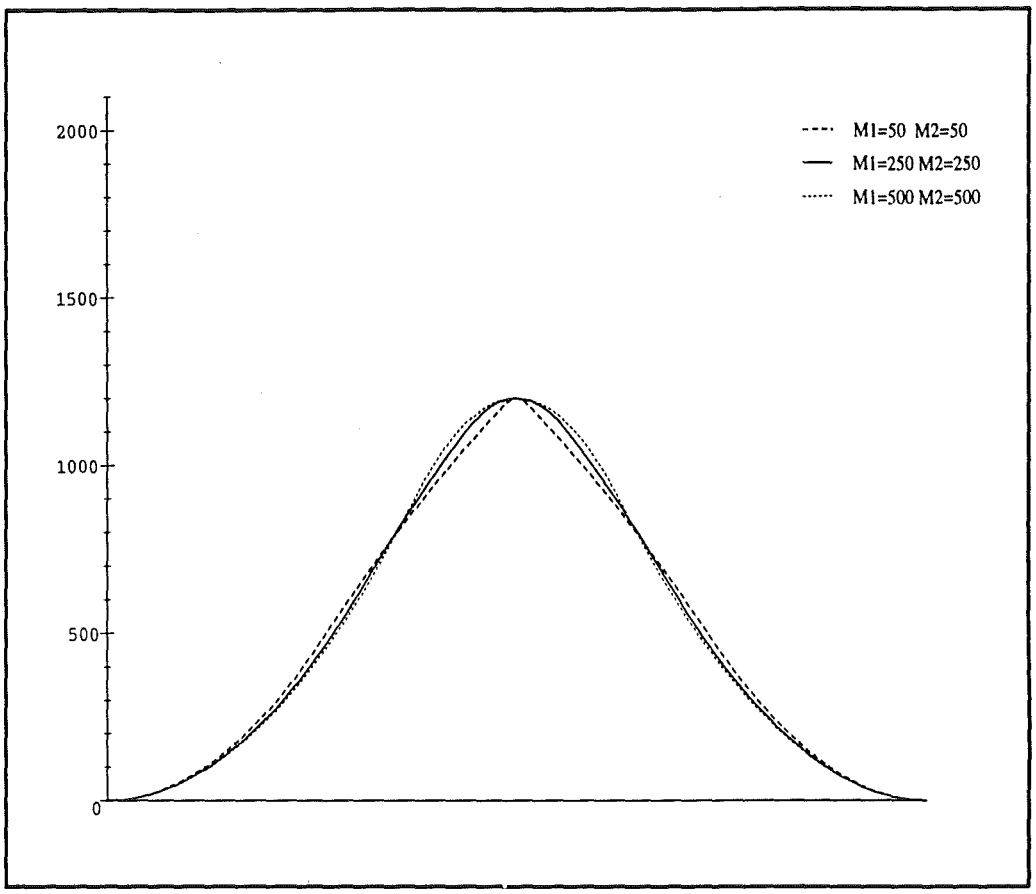

Figure 0.11: Three different shapes for $f(Q|M1 = M2, N1 = N2)$ with $N1 = N2 = 1000$.

Conclusion

Figure 0.12 displays all the possible posterior density functions given the measurements of two pulses when $M1$ and $M2$ have value 100 or 101, and $N1$ and $N2$ have values 1000 or 1001.

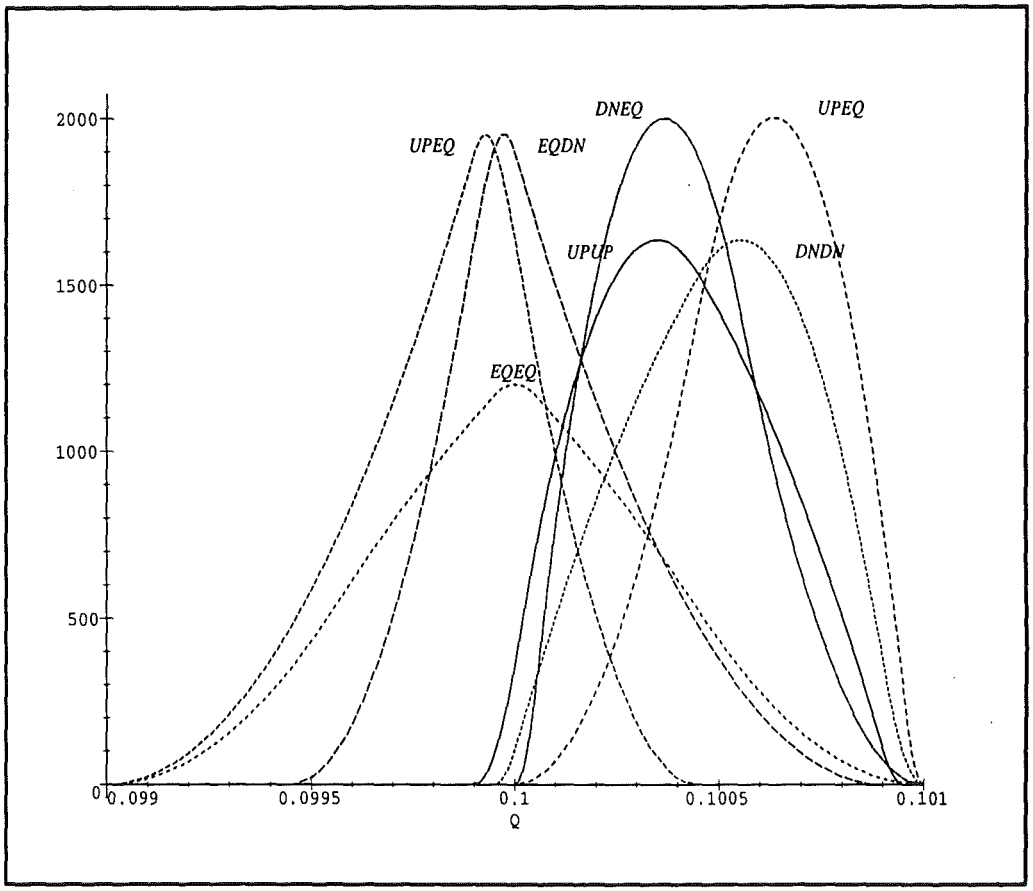

Figure 0.12: The family of all possible posterior densities for τ/T conditioned on a repeated pulse measurement for which M_1 and M_2 have value 100 or 101 and N_1 and N_2 have values 1000 or 1001.

References

Lad, F. and Dunlop, G. R. (1996a) Posterior distribution for the pulse width modulation of a square wave conditional on digital measurements of its on-off components, *University of Canterbury Department of Mathematics and Statistics Technical Report* #134.

Lad, F. and Dunlop, G. R. (1996b) Information Gain for the Pulse Width Modulation of a Square Waveform by Continued Signal Tracking through a Second Pulse, *University of Canterbury Department of Mathematics and Statistics Technical Report* #136.

Appendix A

The regions of the unit cube

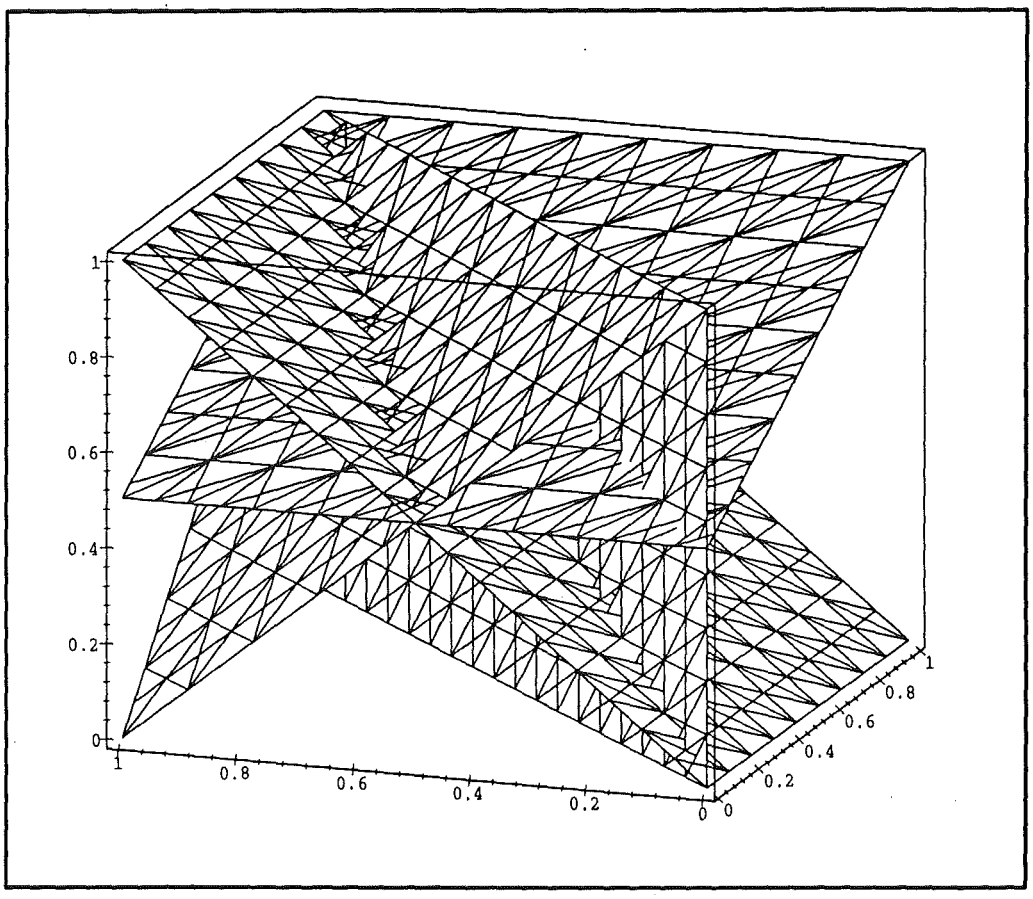

Figure A.1: The unit-cube representing possible values of $\epsilon_0 < \epsilon_\tau < \epsilon_T$ via $x < y < z$, for the regions we designate by 1A1, 1A2, 1A3. The planes defined by $z = (x-1)/2$ and $z = x - y + 1$ determine the bounding Region, by the ordering of $\epsilon_1 = x - z + 1$ between x and y for 1A1, between y and z for 1A2 and between z and 1 for 1A3.

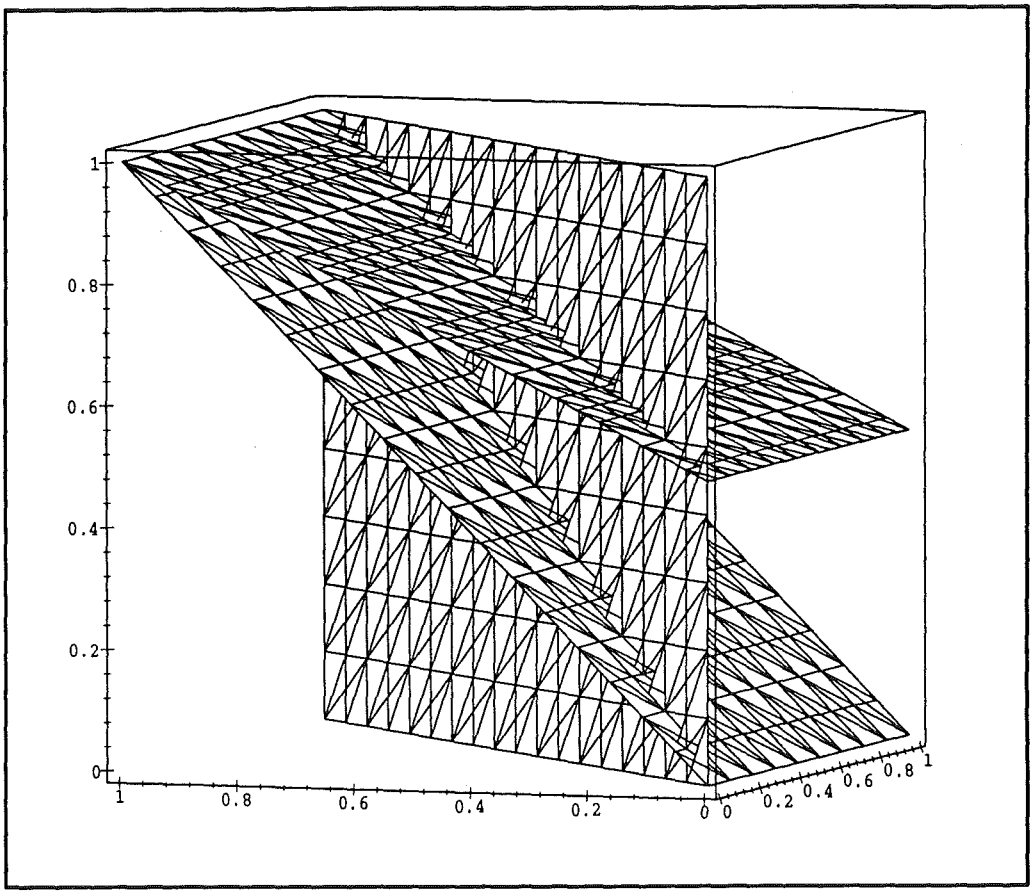

Figure A.2: The unit-cube representing possible values of $\epsilon_\tau < \epsilon_0 < \epsilon_T$ via $x < y < z$, for the regions we designate by 1B1, 1B2. The plane defined by $z = (y + 1)/2$ determines the bounding Region, by the ordering of $\epsilon_1 = y - z + 1$ between y and z for 1B1 and between z and 1 for 1B2.

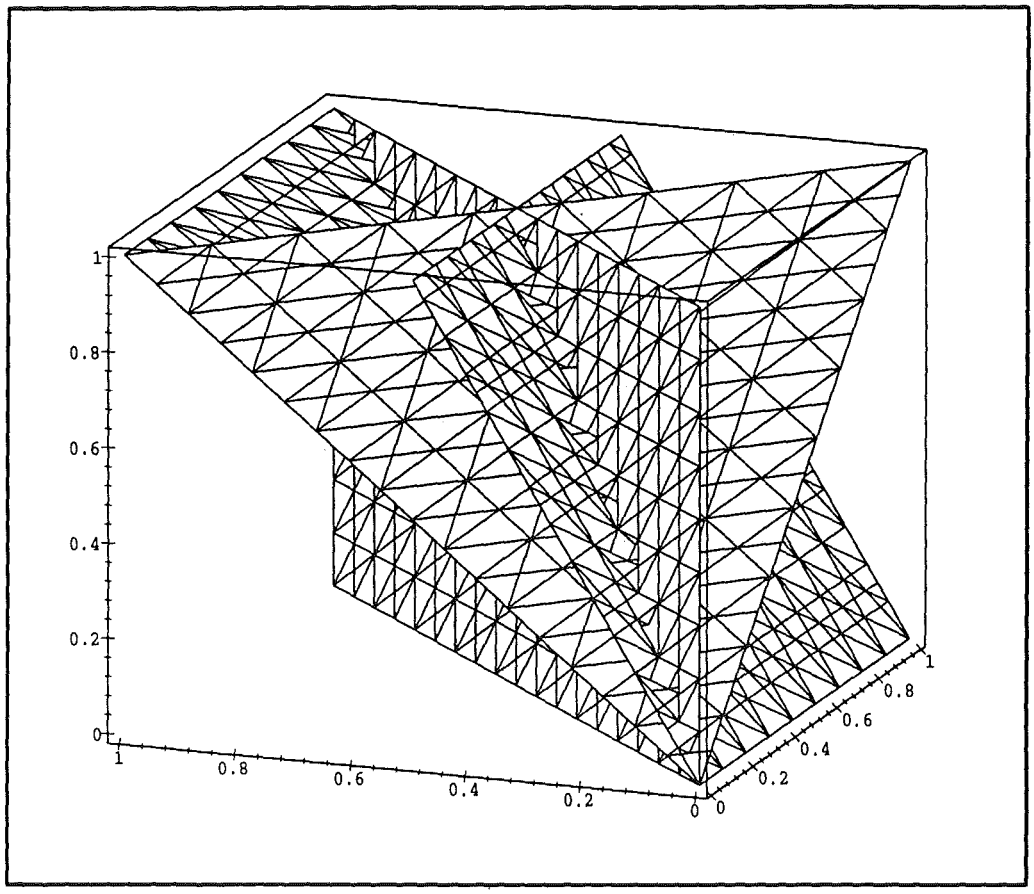

Figure A.3: The unit-cube representing possible values of $\epsilon_\tau < \epsilon_T < \epsilon_0$ via $x < y < z$, for the regions we designate by 1C1, 1C2, 1C3. The planes defined by $z = x + y$ and $z = 2y$ determine the bounding Region, by the ordering of $\epsilon_1 = z - y$ between 0 and x for 1C1, between x and y for 1C2 and between y and z for 1C3.

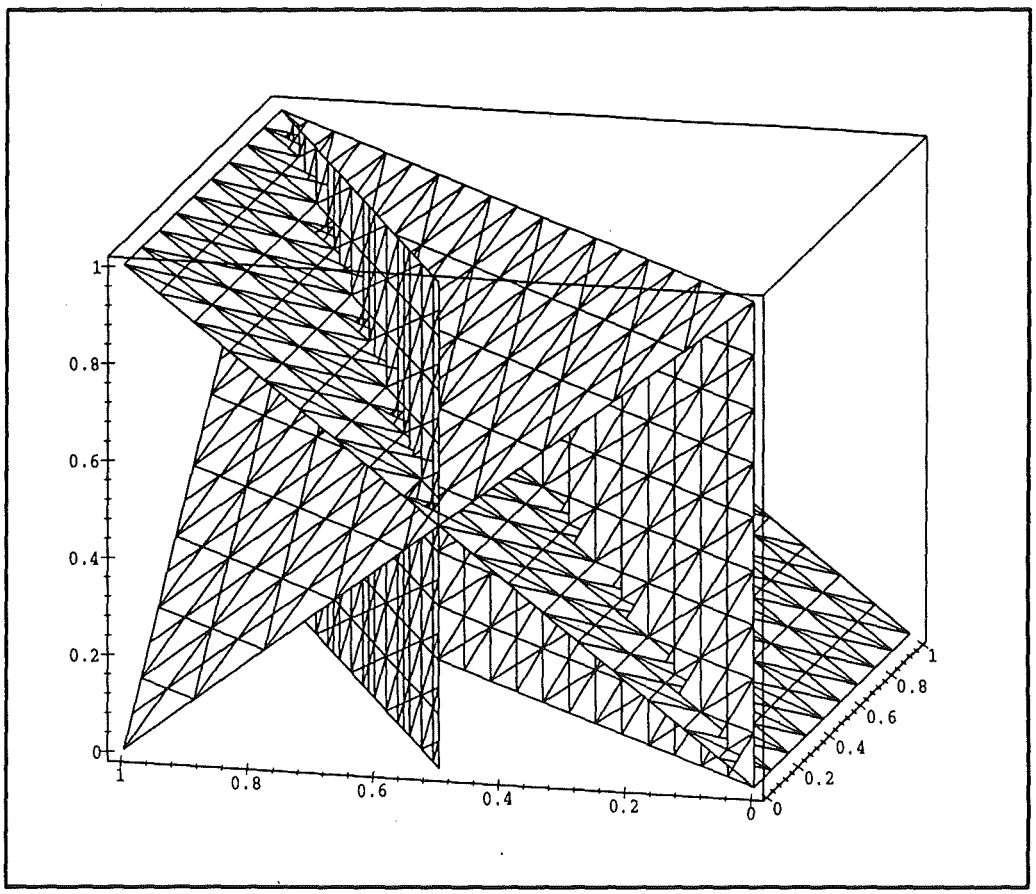

Figure A.4: The unit-cube representing possible values of $\epsilon_0 < \epsilon_T < \epsilon_\tau$ via $x < y < z$, for the regions we designate by 2A1, 2A2, 2A3. The planes defined by $y = (x+1)/2$ and $z = x - y + 1$ determine the bounding Region, by the ordering of $\epsilon_1 = x - y + 1$ between x and y for 2A1, between y and z for 2A2 and between z and 1 for 2A3.

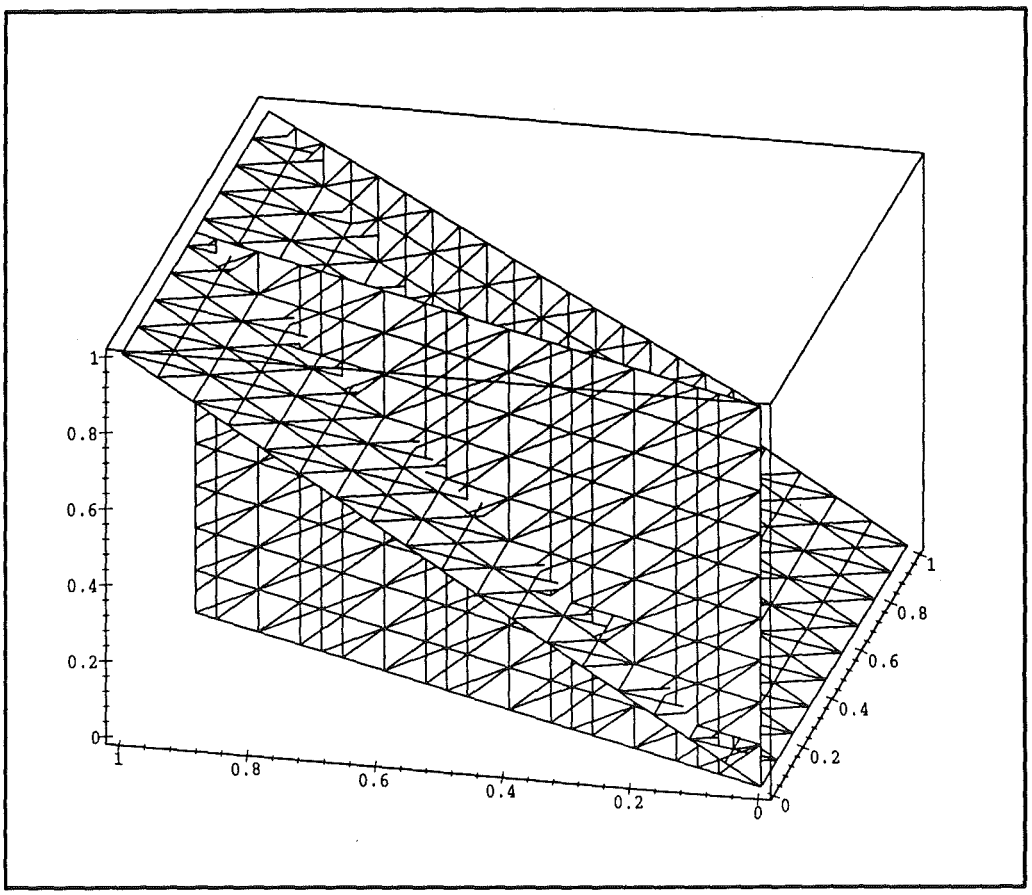

Figure A.5: The unit-cube representing possible values of $\epsilon_T < \epsilon_0 < \epsilon_\tau$ via $x < y < z$, for the regions we designate by 2B1, 2B2. The plane defined by $y = 2x$ determines the bounding Region, by the ordering of $\epsilon_1 = y - x$ between 0 and x for 2B1 and between x and y for 2B2.

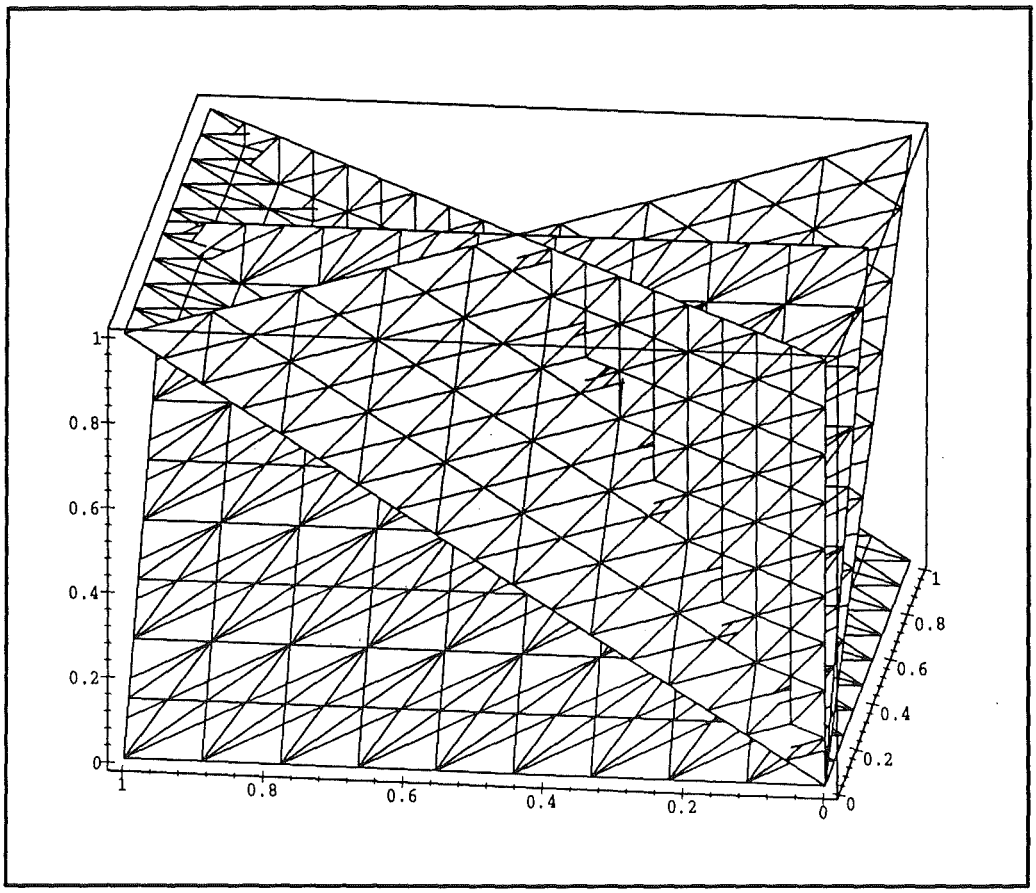

Figure A.6: The unit-cube representing possible values of $\epsilon_T < \epsilon_\tau < \epsilon_0$ via $x < y < z$, for the regions we designate by 2C1, 2C2, 2C3. The planes defined by $z = x + y$ and $z = 2x$ determine the bounding Region, by the ordering of $\epsilon_1 = z - x$ between 0 and x for 2C1, between x and y for 2C2 and between y and z for 2C3.

Appendix B

Category I plots

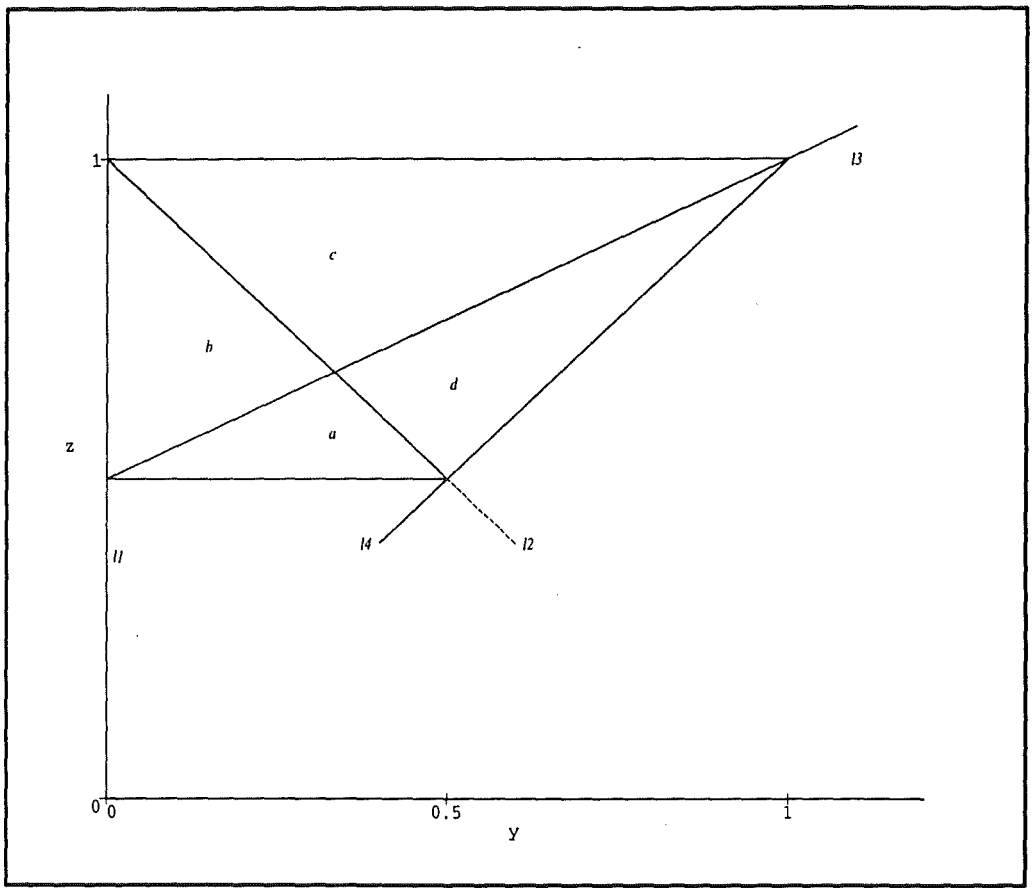

Figure B.1: Projection of Region 1A2 in the space (y, z).

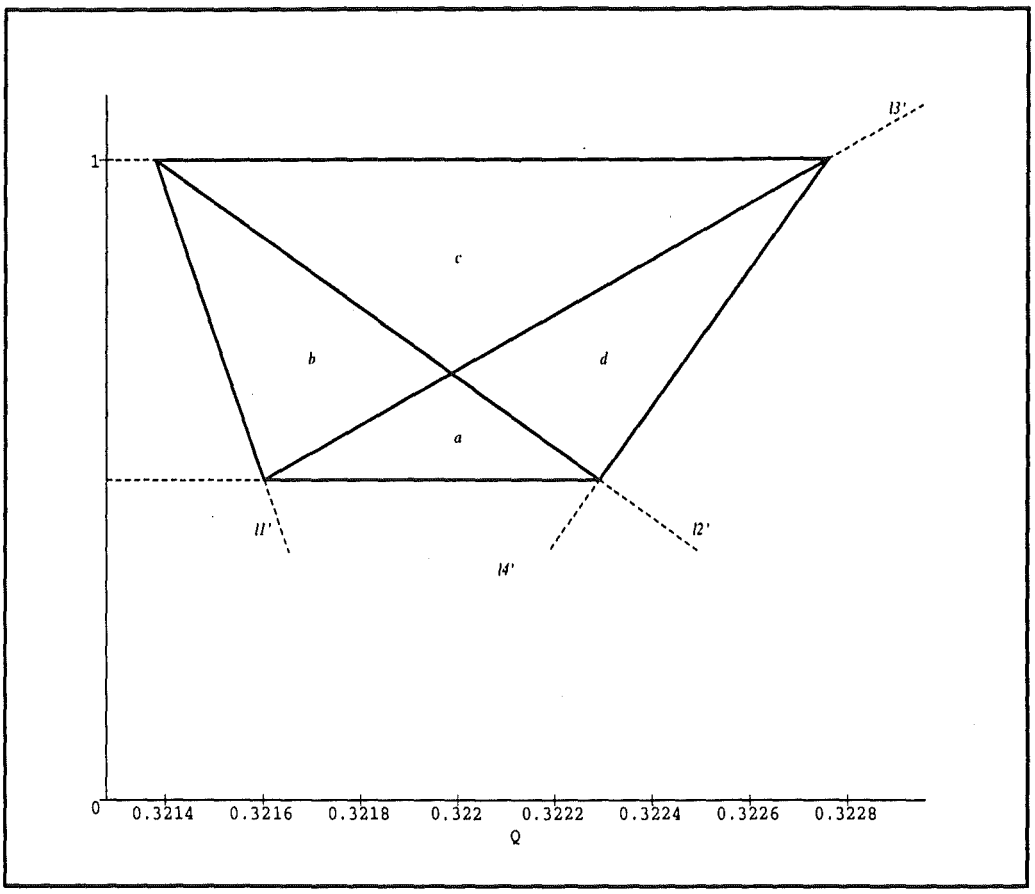

Figure B.2: $T(1A2)$ is a transformation of the domain 1A2 by $(y, z) \longrightarrow (Q, y)$.

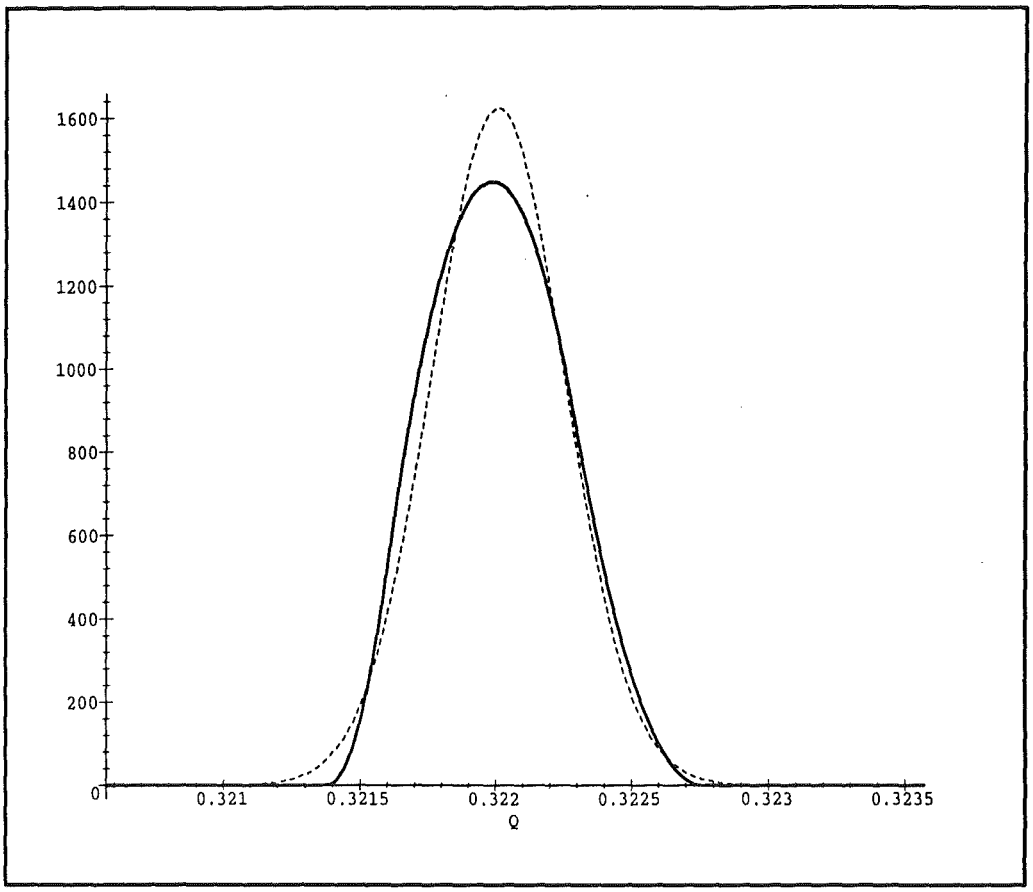

Figure B.3: The density function $f(Q|M1 = 234, M2 = 233 N1 = N2 = 725)$ appears as the solid black curve. For comparative purposes, the dashed curve plots a normal density with the same mean and variance: $N(0.3220075846, 0.603 \cdot 10^{-7})$.

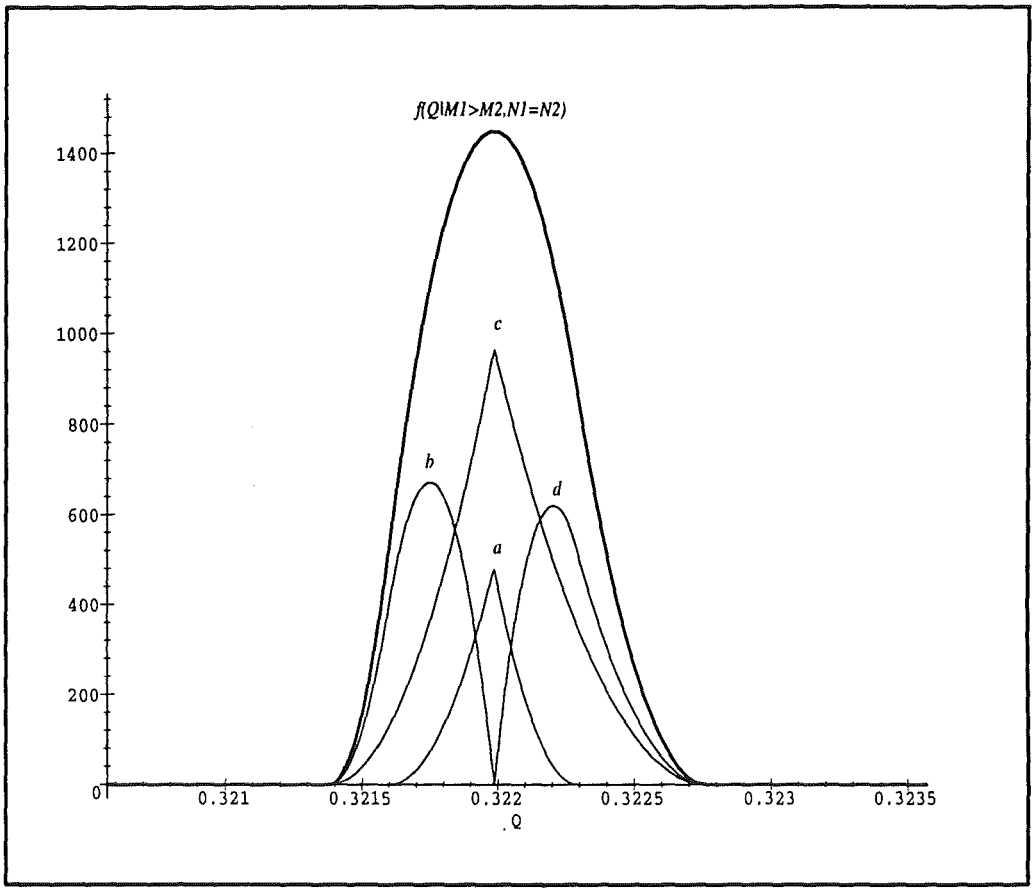

Figure B.4: The density function $f(Q|M1 = 234, M2 = 233, N1 = N2 = 725)$ and the four contributing component functions derived by integrating the joint density over the parts a, b, c, and d of Figure B.2.

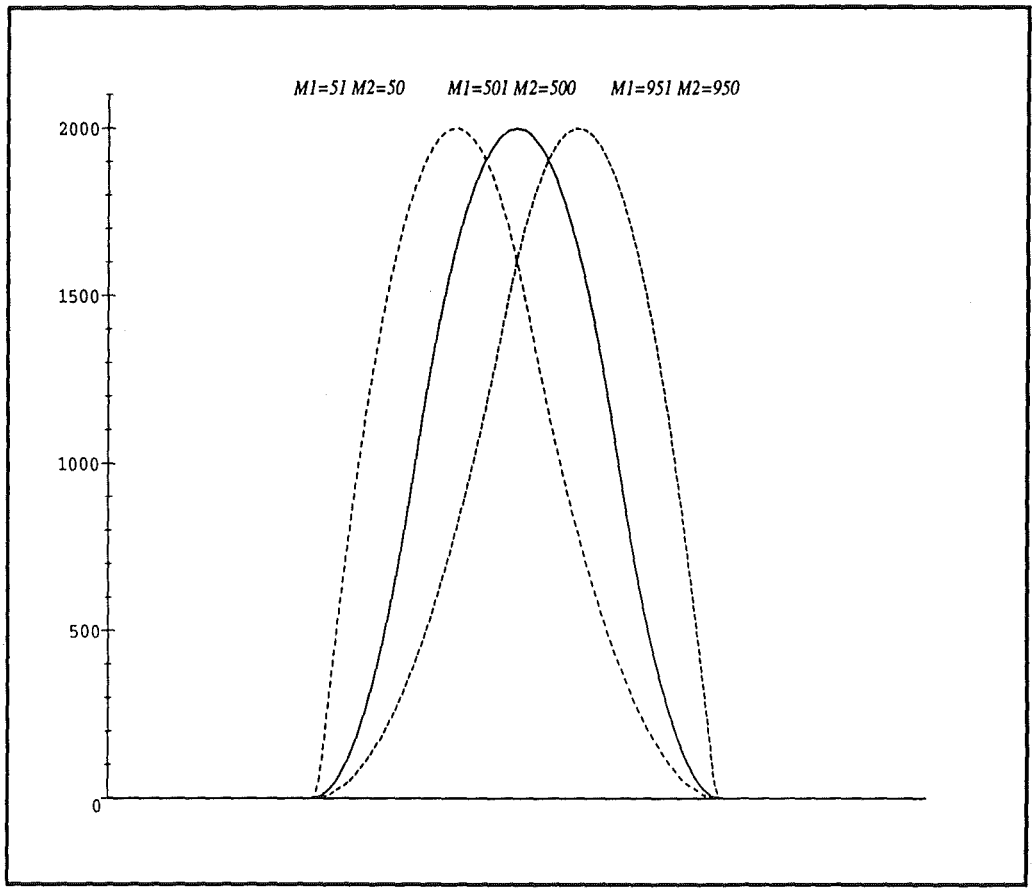

Figure B.5: Three different shapes for $f(Q|M1 > M2, N1 = N2)$ with $N1 = N2 = 1000$.

Appendix C

Categoty II plots

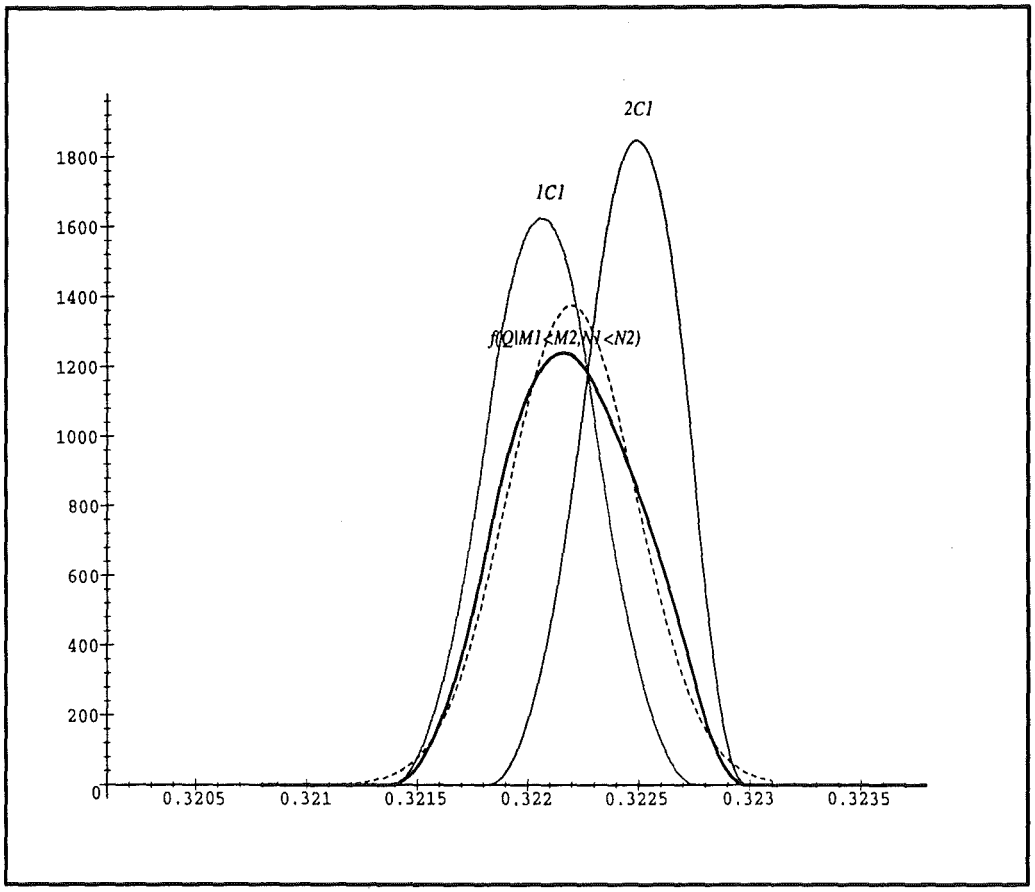

Figure C.1: The density function $f(Q|M1 = 233, M2 = 234, N1 = 724, N2 = 725)$ appears as the fat solid line. The densities conditional within regions 1C1 and 2C1 appear as the thin solid lines, and for comparative purposes, the dashed line plots a normal density.

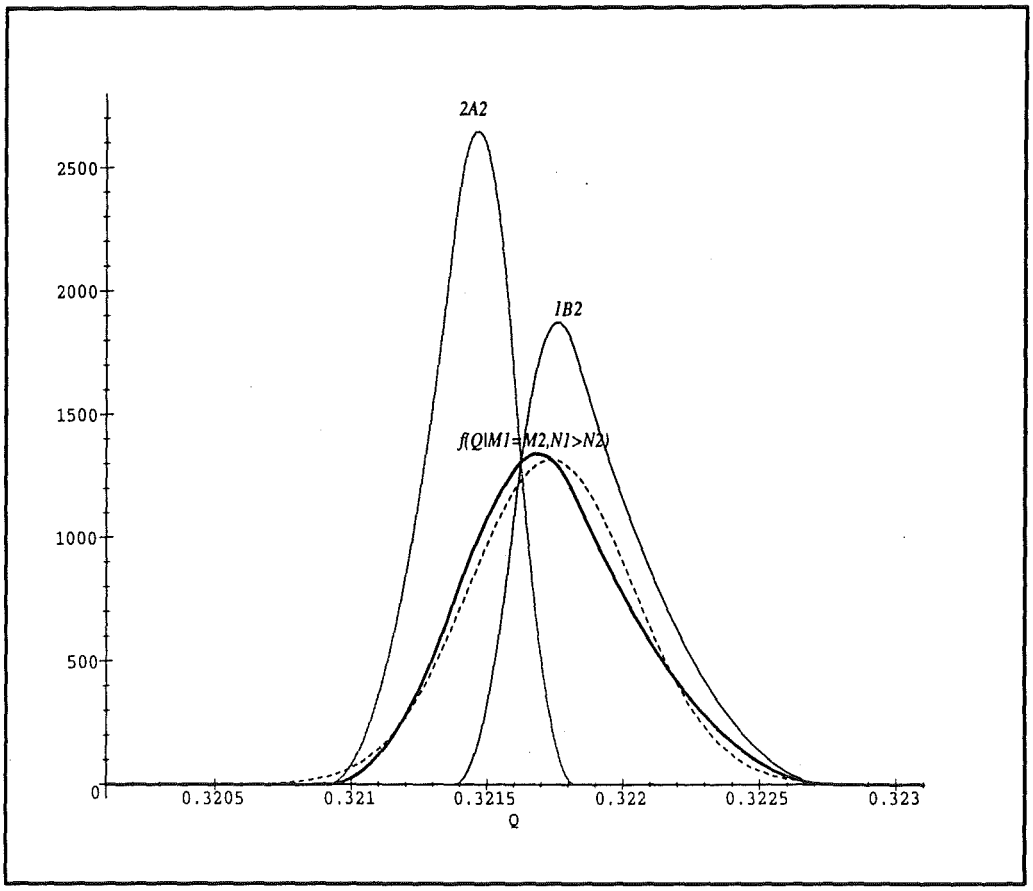

Figure C.2: The density function $f(Q|M1 = M2 = 233, N1 = 725, N2 = 724)$ appears as the fat solid line. The densities conditional within regions 1B2 and 2A2 appear as the thin solid lines, and for comparative purposes, the dashed line plots a normal density.

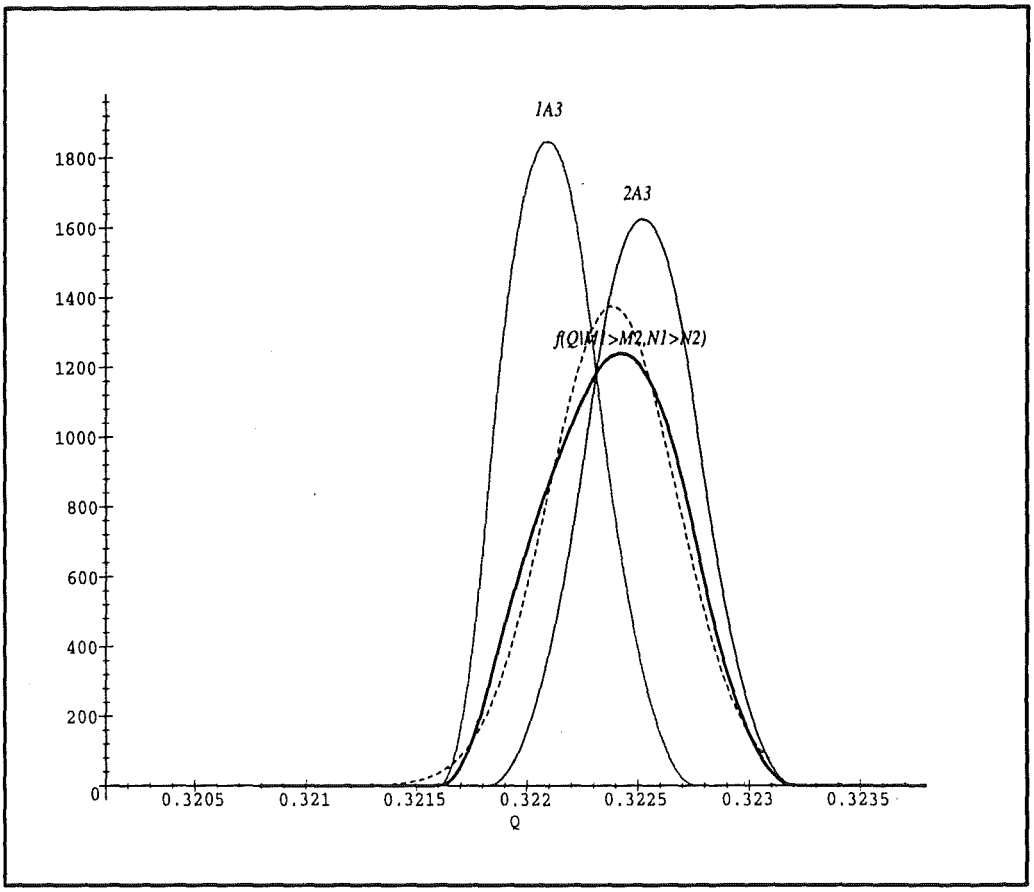

Figure C.3: The density function $f(Q|M1 = 234, M2 = 233, N1 = 725, N2 = 724)$ appears as the fat solid line. The densities conditional within regions 1A3 and 2A3 appear as the thin solid lines, and for comparative purposes, the dashed line plots a normal density.

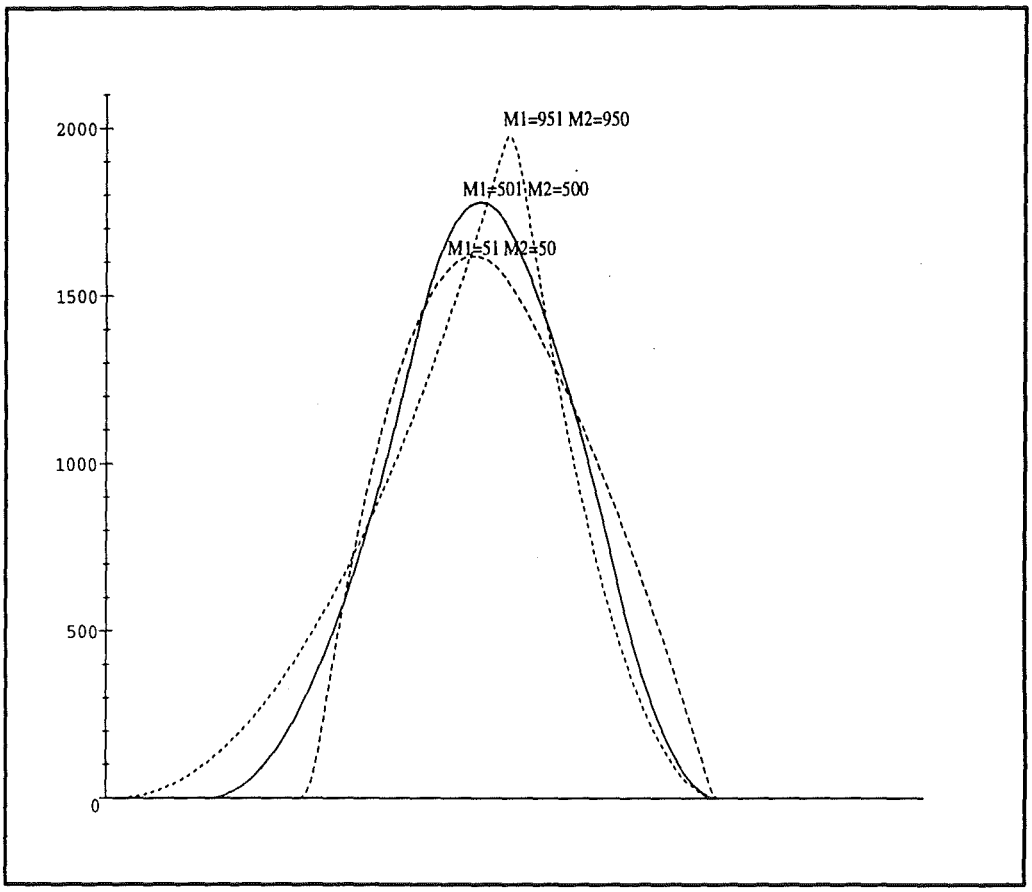

Figure C.4: Three different shapes for $f(Q|M1 < M2, N1 < N2)$ with $N1 = 1000$ and $N2 = 1001$

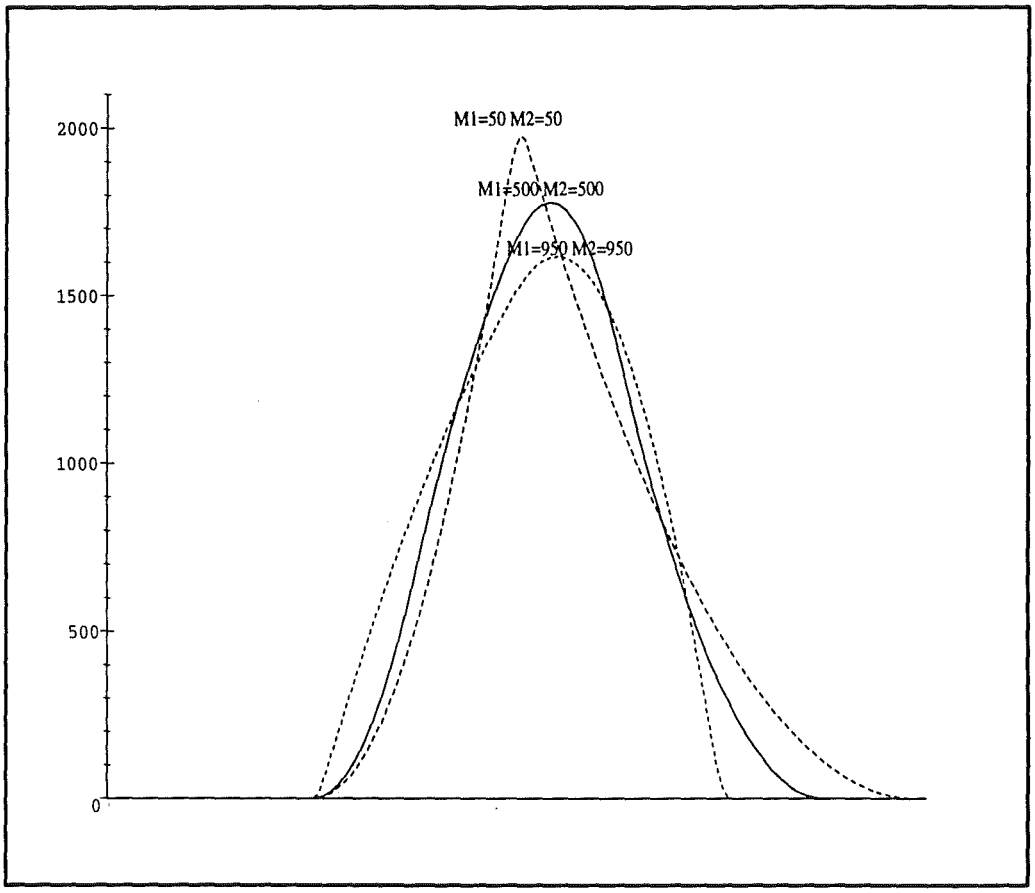

Figure C.5: Three different shapes for $f(Q|M1 = M2, N1 > N2)$ with $N1 = 1001$ and $N2 = 1000$

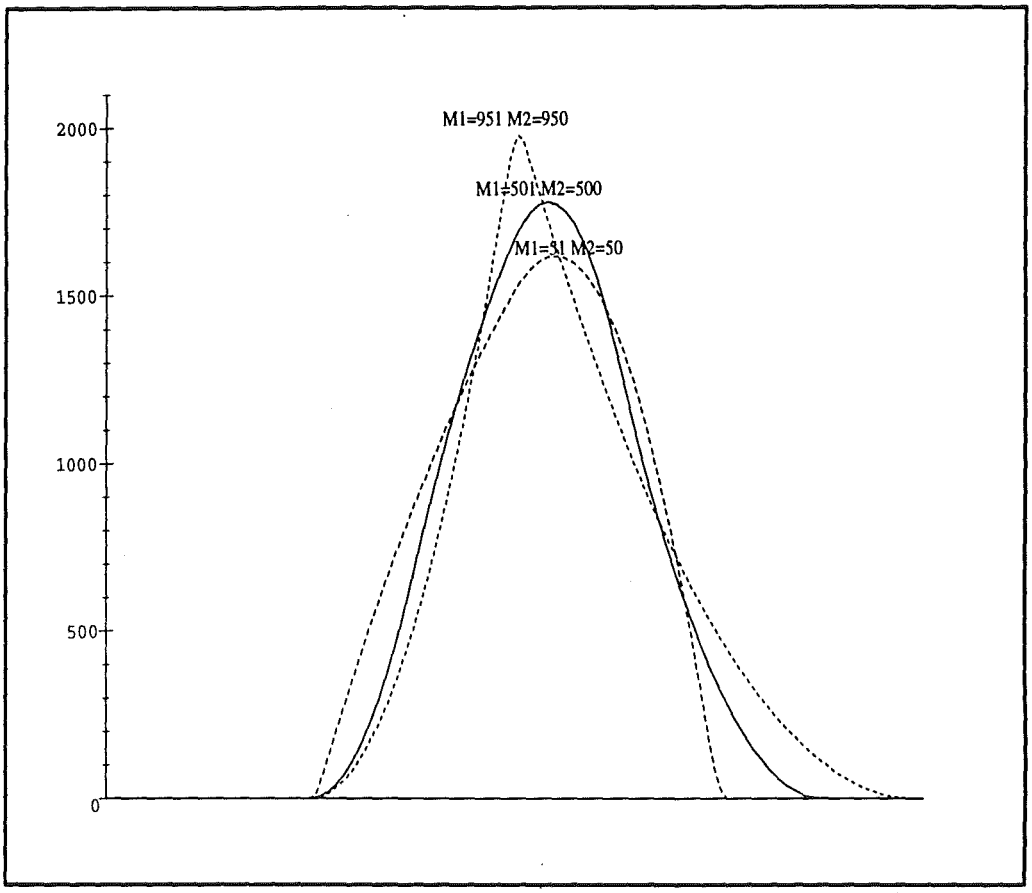

Figure C.6: Three different shapes for $f(Q|M1 > M2, N1 > N2)$ with $N1 = 1001$ and $N2 = 1000$